Comparative Biochemistry and Physiology, Part C 308 (2026) 110633

Contents lists available at ScienceDirect

Comparative Biochemistry and Physiology, Part C

journal homepage: www.elsevier.com/locate/cbpc

Research article

Single and mixtures toxicity of emerging (polystyrene nanoplastic) and persistent (PAHs and PCBs) pollutants and their sub-lethal adverse effects on larval stage zebrafish (*Danio rerio*)

Asif Mortuza [a,*], Daniel Kemp [a], Antonietta Quigg [a,c,d], R.J. David Wells [a,c,d], Karl Kaiser [b], David Hala [a,d], Lene H. Petersen [a]

[a] Department of Marine Biology, Texas A&M University at Galveston, Galveston, TX, 77553, USA
[b] Department of Marine and Coastal Environmental Science, Texas A&M University at Galveston, Galveston, TX, 77553, USA
[c] Department of Oceanography, Texas A&M University, 3146 TAMU, College Station, TX, 77843, USA
[d] Department of Ecology and Conservation Biology, Texas A&M University, 3146 TAMU, College Station, TX, 77843, USA

ARTICLE INFO

Edited by Martin Grosell

Keywords:
Persistent pollutants
Microplastics
Zebrafish
EROD activity
Metabolic rate
Cardiac function

ABSTRACT

Persistent organic pollutants (POPs) such as polycyclic aromatic hydrocarbons (PAHs) and polychlorinated biphenyls (PCBs), with emerging contaminants such as nano-microplastics, continue to raise concerns for both wildlife and human health. This study evaluated the sub-lethal effects of environmentally relevant concentrations of single and mixtures of PAHs, PCBs, in co-exposure with polystyrene (PS) nanoplastics during the early life stages of zebrafish (*Danio rerio*). Larvae ($n = 25$/treatment) were exposed from 2 to 5 days post-fertilization (dpf) in semi-static renewal conditions in temperature (28 ± 1 °C) controlled aquaria. Mixtures of PAHs and PCBs triggered in vivo cytochrome P450 (CYP450) biotransformation activity, which aligned with increases in mass-specific metabolic (oxygen consumption) rate (MO_2). This elevation in MO_2 suggests a heightened requirement for molecular oxygen, likely supporting CYP450-mediated mono-oxygenation pathways. Exposure to PS nanoplastics alone (0.1 μm beads at 10 μg/L) did not significantly alter any measured endpoints. In contrast, co-exposure of PS nanoplastics with either phenanthrene (PHE) or PCB 81 produced 70% and 57% increases in MO_2, respectively. Significant reductions in cardiac blood flow were detected in larvae exposed to PCB 18 + PS, PCB 81 + PS, and PCB 105 + PS, indicating that PCBs co-exposure with PS were the primary contributors to the observed cardiovascular impairments rather than PS nanoplastics alone. Collectively, these results emphasize the value of studying multivariate sub-lethal effects of persistent contaminants (PAHs, PCBs) and emerging pollutants such as nanoplastics in various environmentally relevant concentration mixtures to understand contaminant toxicity.

1. Introduction

Concerns about the potential health impacts of micro and nanoplastic exposure on both wildlife and humans have continued to grow (Kannan and Vimalkumar, 2021; Wei et al., 2022; Li et al., 2023; C.J. Hu et al., 2024; Jeong et al., 2024; Nihart et al., 2025). Research indicates that 60% of marine mammals, 50% of sea birds, and 42% of fish have ingested plastics from the environment (Ugwu et al., 2021). Plastics, first developed in the 1940s, rapidly became widely adopted due to their favorable characteristics, including flexibility, low weight, durability, low cost, and low thermal conductivity (Andrady, 2011). Since their introduction, global plastic production has expanded dramatically from 15 million tons to 335 million tons over the past 70 years (Gall and Thompson, 2015; Dawson et al., 2018). In the environment, plastics undergo slow degradation primarily through photooxidation, thermal oxidation, mechanical abrasion, and microbial action, all of which progressively weaken polymer chains and generate smaller particles (Singh and Sharma, 2008; Chamas et al., 2020; Zhang et al., 2021; Sharma et al., 2022). As these processes proceed, macro-plastics (> 5 mm) fragment into microplastics (1 μm – 5 mm) and nanoplastics (< 1 μm) of diverse shapes and sizes (Qiao et al., 2019; Bermúdez and Swarzenski, 2021).

* Corresponding author.
E-mail address: morta02@tamu.edu (A. Mortuza).

https://doi.org/10.1016/j.cbpc.2026.110633
Received 6 April 2026; Received in revised form 16 July 2026; Accepted 21 July 2026
Available online 23 July 2026

Marine organisms can become entangled in larger plastic items such as discarded fishing gear, plastic bags, and other debris, which can inflict physical injuries and impair essential behaviors such as swimming and foraging (Gregory, 2009; Wang et al., 2023). Moreover, marine species may mistake plastic materials for prey, resulting in ingestion and subsequent internal damage (Sigler, 2014). This threat is particularly pronounced for sea turtles, seabirds, fish, and marine mammals. Once ingested, plastics can obstruct the digestive tract, reduce nutrient uptake, and ultimately lead to malnutrition, starvation, or mortality (Kenyon and Kridler, 1969; Gregory, 2009; Tong et al., 2023; Garcês et al., 2024). Furthermore, smaller nanoparticles (< 1 μm) can traverse through the gut epithelium and penetrate various tissue and affect gut microbiome, enzymatic activity and cell metabolism (Deng et al., 2017; Donkers et al., 2022; Guo et al., 2022; Toto et al., 2022). Documented toxicological effects of microplastics include the induction of oxidative stress (Barboza et al., 2018; Pitt et al., 2018; Liu et al., 2019), altered gene expression (associated with cytochrome and vitellogenin) (Sleight et al., 2017; Qu et al., 2018), genotoxicity (Brandts et al., 2018), changes in neural development (LeMoine et al., 2018), endocrine system disruption Rochman et al. (2014a), neurotoxicity (Barboza et al., 2018), and reproductive abnormalities (Tang et al., 2018). The bioaccumulation and trophic transfer of nano-microplastics (NMPs) and their associated chemicals (plasticizers such as phthalates (e.g., di(2-ethylhexyl) phthalate, DEHP), bisphenol A (BPA), and other bisphenol analogues) can expose higher-level predators including humans to these hazards (Wright et al., 2013; Yang et al., 2015).

Furthermore, plastics can function as carriers of variety of environmental chemicals including flame retardants, persistent organic pollutants (POPs), pesticides, and heavy metals through adsorption to plastic surfaces (Brennecke et al., 2016; Wang et al., 2016). Among the persistent pollutants, polycyclic aromatic hydrocarbons (PAHs) comprise commonly detected pollutants. Low molecular weight PAHs (LMW, ≤3 aromatic rings, petrogenic) are volatile and undergo rapid degradation in the environment (Honda and Suzuki, 2020). In contrast, high molecular weight hydrocarbons (HMW, ≥4 aromatic rings, pyrogenic) exhibit greater environmental persistence and enhanced toxic potency (Incardona et al., 2011). Increases in aromatic ring number (and therefore molecular weight) have been linked to elevated bioaccumulation potential and heightened toxicity (Southworth et al., 1978; Black et al., 1983). PAHs are known to induce a wide range of adverse effects, including metabolic disruption, hemolytic anemia, endocrine disturbances, osmoregulatory impairment, and teratogenic outcomes across diverse taxa (Vandermeulen, 1987; Billiard et al., 2006; Knecht et al., 2013; Incardona and Scholz, 2016; Cunha et al., 2020; Honda and Suzuki, 2020; Sørensen et al., 2020). Polychlorinated biphenyls (PCBs), historically used as dielectric fluids and coolants in electrical equipment, were banned in the late 1970s due to mounting environmental and health concerns (Boyle and Highland, 1979), and are therefore classified as legacy POPs. Despite regulatory restrictions, PCBs continue to be detected in aquatic environments and associated biota because of their long environmental half-lives, and slow degradation rates (Porta and Zumeta, 2002). PCBs and their metabolites can disrupt immune function, impair neurodevelopment, alter endocrine signaling, compromise reproduction, and increase cancer risk in exposed organisms including humans (Sericano et al., 1994; Carpenter, 1998; Winneke et al., 2002; Ulbrich and Stahlmann, 2004; Van den Berg et al., 2006; Goncharov et al., 2011; Hamers et al., 2011; Singleman et al., 2021; Y. Hu et al., 2024).

PAHs, PCBs, and nano-microplastics (NMPs) frequently co-occur in marine environments, making their combined effects an important area of investigation. In this study, the effects of exposure to selected individual PAH and PCB congeners, as well as their mixtures with a model nanoplastic—polystyrene (PS) latex beads (0.1 μm aqueous suspension, density adjusted for freshwater)—were evaluated. Toxicity assessments were conducted using larval zebrafish (*Danio rerio*) as the model organism due to their established use in aquatic toxicology, conserved metabolic pathways, and transparent early-life stages that allow direct visualization of internal organs and physiological responses as part of new approach methodologies (NAM) in environmental toxicology (Tanguay, 2018, 2025). The larvae were exposed from 2 to 5 days post-fertilization (dpf), corresponding to a 72-hour exposure window. Sub-lethal endpoints were measured to characterize physiological responses, including metabolic rate (oxygen consumption), xenobiotic biotransformation activity via ethoxyresorufin-O-deethylase (EROD) assays, and multiple cardiac performance metrics (heart rate, blood flow, and stroke volume). In addition, the nominal plastics exposure concentration selected, i.e., ≤10 μg/L, reflected the surface water concentrations of NMPs that have been quantified in various coastal/estuarine ecosystems along the Gulf of Mexico (Wharton et al., 2024; Gahn et al., 2025; Mortuza et al., 2025). We hypothesized that co-exposure of larval zebrafish to selected PAHs/PCBs and nanoplastics would produce additive or synergistic toxicity relative to exposure to PAHs or PCBs alone. Using environmentally relevant congeners and concentrations (Mortuza et al., 2025), we aimed to characterize the sub-lethal effects of these mixtures at concentrations reflecting their bioaccumulation in exposed biota.

2. Methods

2.1. In vivo toxicity study design using larval zebrafish

Newly fertilized zebrafish (*Danio rerio*) embryos (wild-type, AB strain) were obtained from the Zebrafish International Resource Center (ZIRC) in Eugene, OR. All animal handling and experimental procedures were performed under an approved Institutional Animal Care and Use Committee (IACUC) protocol (2024–0013) at Texas A&M University at Galveston. The toxicological exposure design consisted of exposing larvae at two days post-fertilization (dpf) to selected pollutants or pollutant mixtures for a total duration of three days (72 h), ending at 5 dpf. Fish were maintained under a semi-static renewal regime in which 50% of the exposure medium in each treatment aquarium was replaced daily throughout the experiment. Charcoal-filtered freshwater was sourced from the Sealife Facility at Texas A&M University at Galveston (TAMUG) and used to prepare stock solutions of the chemical mixtures. These mixtures were aerated and maintained at 28 ± 1 °C until their use in the semi-static renewal process. Exposures were conducted in 250 mL glass beakers containing 200 mL of aerated freshwater maintained at 28 ± 1 °C, pH 7.0–7.5, dissolved oxygen > 6 mg/L, nitrite < 0.1 mg/L, nitrate < 10 mg/L, and ammonia < 0.02 mg/L under a 14 h light: 10 h dark cycle, consistent with optimal conditions for zebrafish larvae. Up to 30 larvae were assigned to each chemical treatment.

The single-compound toxicity assays involved exposures to selected PAH and PCB congeners, chosen based on their concentrations and detection frequencies in biota previously collected from Matagorda Bay (plastic production hub) to understand likely sub-lethal mixtures toxicity effects due to their bioaccumulation in exposed biota (Mortuza et al., 2025). Biota body-burden data were used due to the scarcity of PAHs, PCBs, and NMPs data in the surface waters of the area of interest (Matagorda Bay) after Formosa plastic spill (after 2017), and tissue concentrations from our previous work better reflect the mixtures that bioaccumulate in exposed organisms. Specifically, PAHs and PCBs were selected for single-compound or mixture testing only if they accounted for more than 20% of the total body burden in more than 20% of the sampled fish species. The PAHs shortlisted for individual exposures included phenanthrene (PHE; 0.2 μM, 35.65 μg/L), pyrene (PYR; 0.1 μM, 20.23 μg/L), benzo[*a*]anthracene (BaA; 0.6 μM, 136.97 μg/L), and indeno[1,2,3-*cd*]pyrene (IcdP; 0.1 μM, 27.63 μg/L), as summarized in Table 1 and Supplementary Fig. 1. The selected PCB congeners and their exposure concentrations were PCB 18 (0.1 μM, 25.75 μg/L), PCB 81 (0.02 μM, 5.84 μg/L), and PCB 105 (0.04 μM, 13.06 μg/L). Additionally, published LC_{50} values for individual PAHs and PCBs were consulted to ensure that the selected individual contaminant concentrations were

Table 1
A list of the nominal concentrations of single chemical compounds and their mixtures as tested in toxicity studies with 2 dpf larval zebrafish. PS = polystyrene latex beads (0.1 μm) at 10 μg/L final concentration. All groups contain 0.1% DMSO.

Treatments	Without PS	With PS
	Solvent control (0.1% DMSO)	Plastic- PS (polystyrene, 10 μg/L)
PAHs	1. Phenanthrene (0.2 μM, PHE)	1. Phenanthrene (0.2 μM) + PS
	2. Pyrene (0.1 μM, PYR)	2. Pyrene (0.1 μM) + PS
	3. Benzo[*a*]anthracene (0.6 μM, BaA)	3. Benzo[*a*]anthracene (0.6 μM) + PS
	4. Indeno[123-*cd*]pyrene (0.1 μM, IcdP)	4. Indeno[123-*cd*]pyrene (0.1 μM) + PS
PCBs	1. PCB 18 (0.1 μM)	1. PCB 18 (0.1 μM) + PS
	2. PCB 81 (0.02 μM)	2. PCB 81 (0.02 μM) + PS
	3. PCB 105 (0.04 μM)	3. PCB 105 (0.04 μM) + PS
All PAHs + PCBs	1. All PAHs	1. All PAHs + PS
	2. All PCBs	2. All PCBs + PS
	3. All PAHs + PCBs	3. All PAHs + PCBs + PS

well below lethal thresholds, allowing us to observe sublethal effects (Black et al., 1983; Eisler and Belisle, 1996; Verbruggen, 2012; Honda and Suzuki, 2020). Dimethyl sulfoxide (DMSO) was used as the solvent control at 0.1% (v/v) in water and included in all treatment groups to ensure consistent solvent exposure, facilitate dissolution of hydrophobic PAH and PCB congeners, and aid in maintaining uniform suspension of the polystyrene (PS) nanoplastic particles. Stock solutions were prepared in 1-L Erlenmeyer flasks, continuously aerated and maintained in a 28 ± 1 °C water bath; before each semi-static renewal, the mixtures were homogenized using a magnetic stir bar to ensure uniform dispersion. All chemical standards were obtained from Sigma-Aldrich (St. Louis, MO, USA).

Polystyrene (PS) latex beads (0.1 μm; Sigma-Aldrich, Cat. #LB1) were selected as the representative nanoplastic for this study and were used at a final exposure concentration of 10 μg/L. PS was chosen because it is one of the most widely produced plastics and is frequently detected in the tissues of fish and other aquatic organisms (Ding et al., 2018; Assas et al., 2020; Wang et al., 2021; Leslie et al., 2022). The plastic concentration was based on recent studies showing up to 33 μg/L nano-microplastics in Galveston Bay surface water with a median of 12 μg/L (Gahn et al., 2025). Furthermore, Umamaheswari et al. (2021) have shown an aqueous suspension of 10 μg/L PS (0.1 μm) to be readily bioaccumulated by adult zebrafish. The aqueous suspension (density adjust for freshwater) of PS particles, combined with aeration and semi-static renewal of water, ensured that the nanoplastics remained well dispersed throughout the aquaria. In addition to the single-compound toxicity assays, a series of mixture exposures in which each individual PAH or PCB congener was combined with PS nanoplastic particles (10 μg/L) were also conducted. Beyond these pairwise combinations, additional treatments included mixtures containing all selected PAHs or all selected PCBs, as well as All PAHs + PS, All PCBs + PS, a combined All PAHs + All PCBs mixture, and finally an All PAHs + All PCBs + PS mixture. All PAH exposures were conducted concurrently as one batch, all PCB exposures were conducted concurrently as another batch, and the mixture treatments were performed together in a third separate batch, each with its own solvent control. All mixture formulations are summarized in Table 1.

At the end of each exposure period, all larvae were assessed for mortality (at terminal endpoint), and deceased larvae were excluded from analysis that requires live specimen. A subset of ten larvae per treatment group was transferred to a multi-well micro-respirometry plate to quantify oxygen consumption (metabolic rate) over a period of less than three hours. A separate group of five larvae was used to measure key morphological parameters, including overall length, developmental defects (craniofacial area, craniofocal area reduction), and cardiac performance (heart rate, stroke volume, blood flow). The remaining subset of ten larvae was incubated in a solution containing a chromogenic substrate to evaluate xenobiotic metabolic rate (CYP1A activity) using the EROD assay. All subsets were drawn from a single exposure vessel per treatment; these larvae therefore constitute pseudoreplicates within the same vessel. Detailed descriptions of each assay are provided in the sections below.

2.2. Analytical chemistry for PAHs and PCBs quantification in the exposure aquaria

A 1 mL water sample was collected from each treatment group on each day of the exposure trial, with samples taken from each beaker both before and after the semi-static renewal of the exposure aquaria. The samples collected were dried using a LABCONCO FreeZone Bulk Tray freeze dryer (Cat # 7755040). The samples were then spiked with internal standards for PAHs and PCBs (BaP-d_{12} and PCB 65-d_5, each at a final concentration of 2.5 μg/mL) and subsequently reconstituted in dichloromethane (DCM; Sigma-Aldrich, Cat. #34856) to a 40× concentration factor. Blanks comprising of solvent control (0.1% DMSO) were also processed and analyzed similar to the exposure aquaria, and any signal above background was subtracted from the exposure aquaria samples. GC–MS analysis was performed on the water samples to quantify PAH and PCB concentrations, while Py-GCMS/MS was used to measure nanoplastic (PS) levels following an established protocol (Gahn et al., 2025). Measured concentrations of all pollutants were then compared with their corresponding nominal exposure levels to verify accuracy of the dosing treatments.

2.3. The assessment of zebrafish body morphometry and cardiovascular physiology

A subset of larvae from each treatment group ($n = 5$) was used to assess a range of morphometric and functional parameters. Images and videos of individual fish were captured using an electric stereo microscope (ZEISS SteREO Discovery V8, Germany) equipped with a Basler camera and Pylon Viewer software (version 7.4.0.14900; Ahrensberg, Germany). Morphometric parameters—including total length, craniofacial area, and craniofocal area—were quantified alongside cardiovascular performance metrics including heart rate (beats/min) and arterial blood flow activity (% blood flow) using DanioScope software (version 1.2.206; Noldus Inc., Netherlands). Net mortality was also noted per treatment group at the end of the exposure period. Heart rate was determined by identifying the area of the heart within the software, which then measured the change in pixel per minute (of the captured video) to calculate heart beat (Noldus, 2025). Similarly, arterial flow activity was quantified by measuring the percent change in pixel (proportional to blood flow) within the selected artery exiting the heart, providing a proxy for blood-flow rate (Noldus, 2025).

To calculate Stroke Volume (volume of blood pumped from the ventricle per beat), the volume of the heart ventricle was determined using the videos captured from the Zeiss microscope analysis. Images of the ventricle in systole (contraction of heart muscles) and diastole (relaxation of heart muscles) were used to measure the surface area of the ventricle (at systole and diastole). The heart volume at systole and diastole was subsequently determined using the following formula (where: HV = heart volume, L= longitudinal length, W= latitudinal width) (Hoage et al., 2012; Naderi et al., 2024):

$$Heart\ Volume\ (HV) = \frac{\pi}{6} \times L \times W^2$$

Finally, the cardiac volume at systole and diastole were used to calculate the Stroke Volume (in μL) using the following formula (where: SV= stroke volume, EDV= end diastolic volume, ESV= end systolic volume) (Hu et al., 2001; Bruss and Raja, 2025):

$$Stroke\ Volume\ (SV) = EDV - ESV$$

At the conclusion of each experiment, all larvae were humanely euthanized via cold-stunning in an ice bath (4 °C), followed by cervical severing, in accordance with an approved IACUC protocol.

2.4. EROD assay

A subset of larvae from each treatment group ($n = 10$) was used to quantify pollutant biotransformation capacity using the EROD assay. This assay measures the activity of the Phase I xenobiotic-metabolizing enzyme CYP1A1, which plays a central role in the biotransformation of contaminants such as PAHs and PCBs (Nilsen et al., 1998; Whyte et al., 2000; Noury et al., 2006). The procedure followed the protocol described by Noury et al. (2006). Briefly, ten larvae from each treatment were transferred into individual wells of a 12-well plate, each containing 2 mL of 1.5 μM 7-ethoxyresorufin (ER), the fluorogenic substrate for the assay. The conversion of ER to its fluorescent product, resorufin, via CYP1A1 catalytic activity, was quantified after a 4-h incubation using a fluorescence plate reader. Resorufin was detected at 587 nm with excitation at 545 nm (Noury et al., 2006). All measurements were calibrated against a 12-point resorufin standard curve ranging from 2 μM to 0.001 μM. At the conclusion of each experiment, all larvae were humanely euthanized via cold-stunning in an ice bath (4 °C), followed by cervical severing, in accordance with an approved IACUC protocol.

2.5. Metabolic rate assessment using micro-respirometer

The oxygen consumption rate of 5 dpf larval zebrafish (i.e., at test termination) was measured using a 24-well micro-respirometry system (Loligo® Systems; Viborg, Denmark). This system quantifies dissolved oxygen via optical fluorescence within gas-tight 1.7 mL wells. Individual larvae were placed into separate wells to record changes in oxygen concentration over time. Each well contained an integrated oxygen sensor that was calibrated prior to use with 10% sodium sulfite in deionized water (0% oxygen saturation) and fully aerated water (100% saturation). For each treatment, ten larvae were loaded into individual wells, while four additional wells containing only water served as blanks for baseline oxygen measurements. Larvae were allowed a 30-minute acclimation period before recording began. Oxygen levels in each well were then monitored for up to 3 h to determine metabolic rate across treatments. At the end of the assay, larvae were humanely euthanized by cold-stunning in an ice bath (4 °C), in accordance with an approved IACUC protocol. Euthanized fish were subsequently frozen and later dried in pre-weighed weigh boats for 24 h at 0.20 mbar vacuum and −80 °C using a LABCONCO freeze dryer. The dried larvae were weighed (including the weigh boat) using a Sartorius Cubis microbalance (model CPA2P) to determine dry mass, which was used to calculate mass-specific metabolic rate (MO_2).

Measurement of oxygen consumption provides an estimate of whole-organism bioenergetics, or metabolic rate (Fry, 1971; Lapointe et al., 2014). This parameter reflects the organism's capacity to allocate energy toward essential functions such as survival, growth, and locomotion, and is therefore widely used as an indicator of physiological performance and fitness (Brett, 1964; Priede, 1985; Reidy et al., 2000; Pettersen et al., 2016, 2018; Somero et al., 2017). Mass-specific metabolic rate (MO_2) was calculated using the equation adapted from Petersen and Gamperl (2010):

$$MO_2 = \left[\left(\left(C_i - C_f\right) \times V_c\right) \times 60\right] \times (m \times t)^{-1}$$

where C_i is the initial dissolved oxygen concentration (mg O_2/L), C_f is the final concentration (mg O_2/L), V_c is the respirometer chamber volume (L), m is the dry mass of the fish (kg), and t is the duration of the measurement (min). Resulting MO_2 values, originally expressed as mg O_2/kg/min, were converted to μg O_2/mg/h to facilitate comparison with previously published studies on larval zebrafish (Barrionuevo and Burggren, 1999; Bagatto et al., 2001; Barrionuevo et al., 2010).

2.6. Statistical analysis

Statistical analyses were performed in R (v4.1.3) using the *tidyr* and *ggplot2* packages (Wickham, 2016; Wickham et al., 2024; R, 2025). Data normality was assessed using the Shapiro–Wilk test, followed by Levene's test to evaluate homogeneity of variances. For pairwise comparisons between treatment vs treatment + PS (e.g., between PCB 81 vs PCB 81 + PS) either a parametric *t*-test or a non-parametric Mann-Whitney *U* test was applied, depending on data distribution. For datasets involving solvent control vs treatment and treatment + PS (e.g., PCB 81, PHE, etc. with and without PS) ANOVA was used for parametric data, followed by Tukey's post hoc test. For non-parametric data, group differences were evaluated using the Kruskal-Wallis test, with Dunn's post hoc test applied for pairwise comparisons where appropriate. Statistical significance was defined as $p < 0.05$.

To classify mixture interactions as additive, synergistic, or antagonistic, the Bliss Independence (independent action) model was applied (Bliss, 1939). For each endpoint, individual treatment effects were expressed as fractional changes relative to the solvent control ($f = [E_{treatment} - E_{control}] / E_{control}$), and the predicted combined effect was calculated as $f_{AB} = f_A + f_B - (f_A \times f_B)$, where f_A and f_B represent the fractional effects of the single compound and PS, respectively. The predicted additive mixture response was back-transformed as $E_{predicted} = E_{control} \times (1 + f_{AB})$. Observed mixture responses exceeding the Bliss prediction were classified as synergistic, and those falling below as antagonistic, with strict additivity indicated by no significant departure from the predicted value. The significance of each deviation ($\Delta = E_{observed} - E_{predicted}$) was assessed using a one-sample t-test, and significance was defined as $p < 0.05$. Principal component analysis (PCA) was conducted using the *prcomp* function with variable standardization, resulting in a correlation-based PCA. The PCA results were visualized as a biplot using *ggplot2*. For multivariate correlation analyses, non-parametric Spearman rank correlations were performed, with significance set at $p < 0.05$.

3. Results

3.1. Exposure aquaria treatment concentrations

The overall actual chemical concentrations across the treatment groups varied from 0.4% (for PCB 18) to 20.3% (for BaA) (Supplementary Table 1). The measured concentrations for each compound in the aquaria water were: 0.89 ng/mL (0.0050 μM) for PHE, 0.81 ng/mL (0.0040 μM) for PYR, 27.85 ng/mL (0.122 μM) for BaA, 3.04 ng/mL (0.0110 μM) for IcdP, 0.10 ng/mL (0.00039 μM) for PCB 18, 0.15 ng/mL (0.00051 μM) for PCB 81, and 0.88 ng/mL (0.0027 μM) for PCB 105 (Supplementary Table 1). These exposure levels, i.e., min – max of 0.81–27.85 ng/mL for PAHs; and 0.1–0.88 ng/mL for PCBs, were within range of dissolved total PAHs (0.01–17.05 ng/mL) and PCBs (0.046–0.312 ng/mL) measured in the surface waters of various estuarine ecosystems (Rifai and Palachek, 2007; Lakshmanan et al., 2010; Howell et al., 2011; Williams et al., 2017; Bacosa et al., 2020).

All individual contaminant exposure levels tested were well below their respective literature LC_{50} values both at nominal and actual concentrations, confirming that treatments were within the sublethal range (Black et al., 1983; Eisler and Belisle, 1996; Monosson, 2000; Verbruggen, 2012; Honda and Suzuki, 2020). For example, (Supplementary Table 2) PYR LC_{50} is approximately 0.02 μM (5× lower than the actual concentration tested). BaA LC_{50} is 1.09 μM versus a nominal concentration of 0.6 μM (1.8× lower) and actual concentration of 0.12 μM (9× lower). IcdP LC50 is >1.29 μM, compared to 0.1 μM nominal (12.9× lower). PCB 18 LC50 is 0.33 μM versus 0.1 μM nominal (3.3× lower). These comparisons demonstrate that actual exposure levels were far below acute toxicity thresholds while remaining within environmentally relevant levels.

3.2. Exposure effects on morphometric parameters

Exposure of larval zebrafish to the selected pollutants resulted in a statistically significant reduction in total length relative to the solvent control (0.1% DMSO) only for the BaA + PS mixture ($p = 0.01$) (Table 2). The mean length of larvae in the solvent control group (3.9 ± 0.03 mm) falls within the expected range for ~5 dpf zebrafish, which typically measure under 5 mm at this developmental stage (Singleman and Holtzman, 2014).

For dry weight, exposure to BaA alone resulted in a statistically significant 58% increase in body mass relative to the solvent control (0.1% DMSO). Exposure to IcdP or IcdP + PS also significantly elevated body weight, by 59% and 53%, respectively (Table 2). PCB 105 similarly produced a significant 31% increase in body weight compared to the solvent control. In contrast, co-exposure to PCB 81 + PS and PCB 105 + PS significantly reduced body weight by 43% and 29%, respectively (Table 2). Finally, larvae exposed to the All PAHs mixture alone exhibited a 63% reduction in body weight relative to the solvent control group (Table 2).

Craniofacial developmental defects were observed (Fig. 1) in treatment groups PCB 81, All PCBs, All PAHs + PCBs and All PAHs + PCBs + PS. Fish exposed to BaA and BaA + PS exhibited the greatest reductions in lateral ocular area (−22% and − 30%) and lateral craniofacial area (−14% and − 17%), both significantly smaller compared to the solvent control (0.1% DMSO). PCB 81 + PS, All PAHs + PCBs, and All PAHs + PCBs + PS also showed reductions in ocular (−11%, −19%, −16%) and craniofacial area (−17%, −9%, −12%), though these differences were not statistically significant compared to the solvent control. In terms of mortality, All PAHs + PCBs and All PAHs + PCBs + PS groups showed 100% (represented in Fig. 1c) mortality on the second day of exposure. PCB 81 and PCB 81 + PS showed 23% and 27% mortality respectively at test termination. Control groups showed no mortality. Sub-lethal endpoints were not assessed for groups exhibiting 100% mortality.

Table 2
Total length (n = 5) and dry weight (n = 10) of zebrafish exposed to single compounds and/or mixtures of a) PAHs (+PS), b) PCBs (+PS), and c) combined PAHs, PCBs, and PS. Asterisks (*p < 0.05, **p < 0.01, ***p < 0.001) indicate significant differences from the solvent control, whereas different letters denote significant differences among treatment groups with and without PS.

Treatments	Length (mm)		Weight (mg)	
	Without PS	With PS	Without PS	With PS
PAHs				
Solvent control	3.92 ± 0.03	3.94 ± 0.03	0.02 ± 0.00	0.02 ± 0.00
PHE	3.95 ± 0.04	3.97 ± 0.03	0.01 ± 0.00	0.01 ± 0.00
PYR	3.82 ± 0.04	3.89 ± 0.06	0.02 ± 0.00	0.04 ± 0.00
BaA	3.75 ± 0.07	3.67 ± 0.06**	0.05 ± 0.01***	0.04 ± 0.01
IcdP	3.82 ± 0.03	3.81 ± 0.05	0.05 ± 0.00***	0.04 ± 0.00*
PCBs				
Solvent control	3.85 ± 0.02		0.05 ± 0.00	
PCB 18	3.86 ± 0.04	3.83 ± 0.04	0.07 ± 0.00	0.06 ± 0.01
PCB 81	3.80 ± 0.06	3.68 ± 0.07	0.07 ± 0.01 a	0.04 ± 0.00* b
PCB 105	3.91 ± 0.04	3.88 ± 0.02	0.07 ± 0.01** a	0.05 ± 0.00 b
All PAHs/PCBs				
Solvent Control	3.74 ± 0.06		0.02 ± 0.00	
All PAHs	3.74 ± 0.03	3.77 ± 0.02	0.02 ± 0.00	0.02 ± 0.00
All PCBs	3.75 ± 0.06	3.65 ± 0.03	0.01 ± 0.00***	0.01 ± 0.00

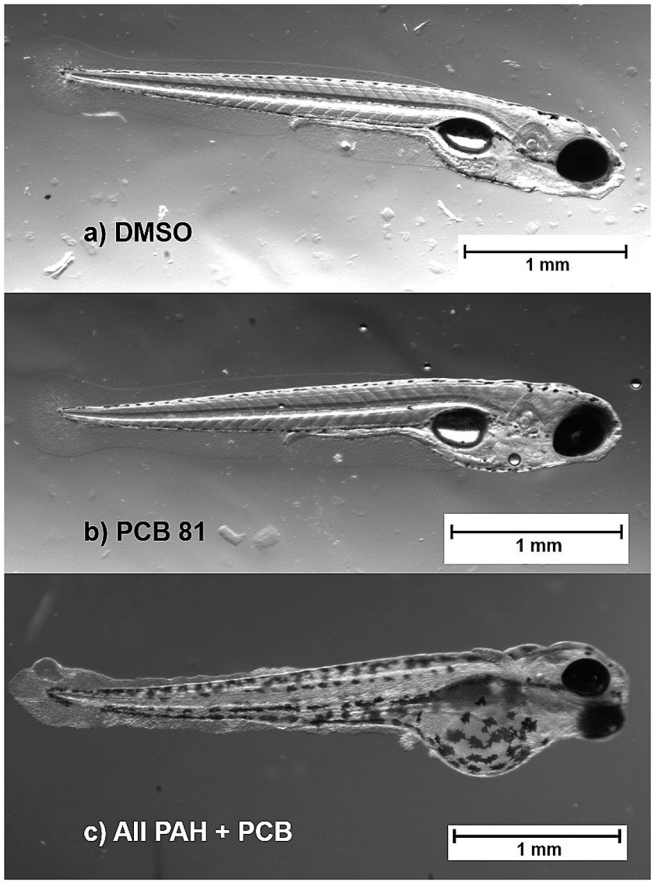

Fig. 1. Images of representative larval zebrafish (5 dpf, 65× magnification) exposed to a) solvent control (DMSO), b) PCB 81 and c) all PAH + PCB, illustrating reduced craniofacial area in both b) and c) as well as fin malformation and pigmentation in c). The larvae represented in c) are deceased.

3.3. Exposure effects on mass specific EROD activity

Because the EROD activity dataset contained pseudo-replication, statistical comparisons were not performed; instead, a single mean value was calculated for each treatment group. Consequently, EROD responses were evaluated qualitatively using multivariate PCA (Fig. 2) and correlational analysis with MO_2 (Fig. 3). Even without formal statistical testing, several clear trends emerged. For the PAH exposures, both PHE and PHE + PS induced elevated EROD activity, showing 59% and 57% increases, respectively, relative to the solvent control (Table 3). Among the PCB treatments, larvae exposed to PCB 81 + PS exhibited a 51% increase in EROD activity compared to the solvent control (Table 3). Across the mixture treatments, all groups containing combined PAHs or PCBs showed higher EROD activity than the solvent control. The All PCBs mixture produced the strongest response, with an 80% increase in activity. The All PAHs mixture resulted in a 48% increase, while the All PAHs + PS group showed a 52% elevation. Larvae in the All PCBs + PS treatment exhibited a 44% increase in EROD activity relative to the solvent control (Table 3).

3.4. Exposure effects on mass specific metabolic rate (MO_2)

Overall, the MO_2 patterns observed across single-compound and mixture exposures closely mirrored the trends reported for mass-specific EROD activity (Table 3; Fig. 3). Among the PAH treatments, PHE and PHE + PS produced 46% (statistically significant) and 70% (not significant) increases in metabolic rate, respectively, relative to the solvent control. The lack of statistical significance for the PHE + PS group likely

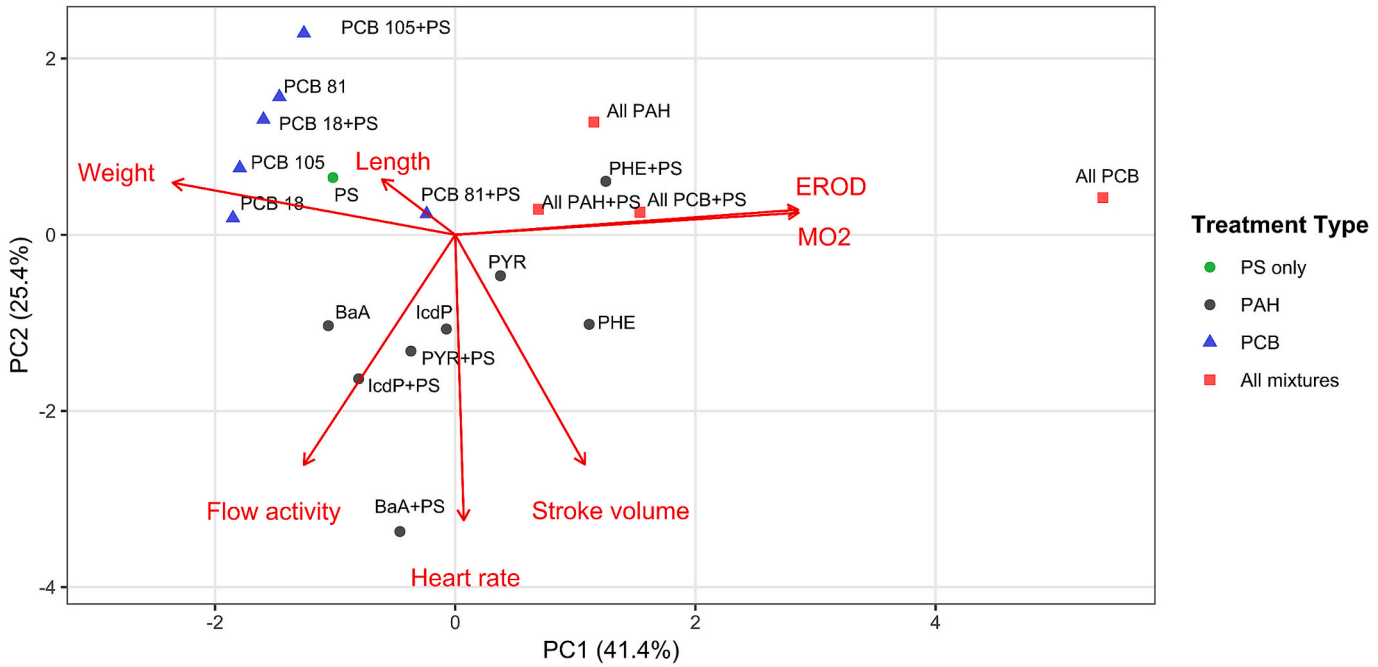

Fig. 2. Principal component analysis (PCA) biplot illustrating the overall relationships between single-compound and mixture treatments of PAHs, PCBs, and PS, and the corresponding sub-lethal effects measured in exposed larval zebrafish.

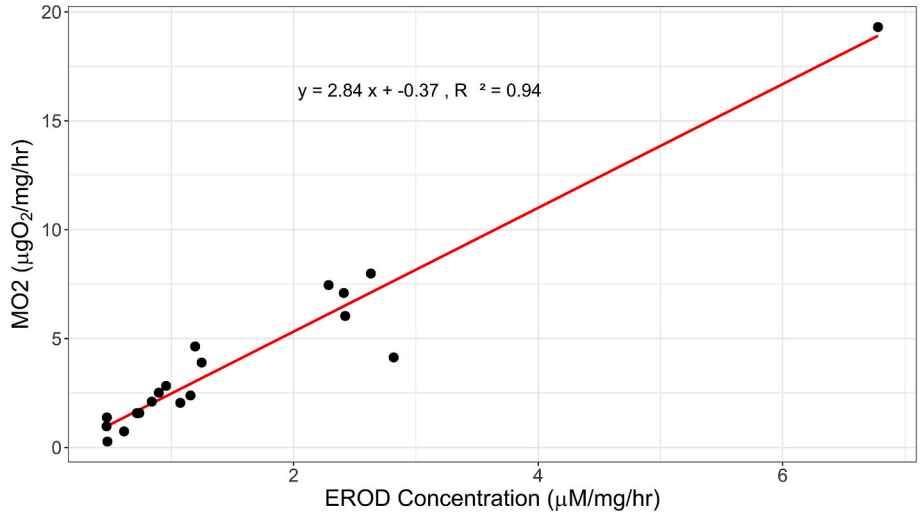

Fig. 3. Correlational analysis illustrating the relationship between mass-specific metabolic rate (MO_2) and EROD activity in larval zebrafish exposed to PAHs, PCBs, and/or PS mixtures.

reflects its higher variability (98% coefficient of variation) compared with the PHE-only group (50% CV). Consistent with the EROD results for PCB exposures, larvae in the PCB 81 + PS group exhibited a 57% increase in MO_2 relative to the solvent control, although this difference was not statistically significant due to substantial variability (~78% CV) (Table 3). Finally, in agreement with the strong EROD response observed for the All PCBs mixture, larvae exposed to this treatment showed a statistically significant 84% increase in MO_2 compared to the solvent control. In contrast, the All PCBs + PS group exhibited a significant 47% reduction in MO_2 relative to the All PCBs-only treatment (Table 3).

3.5. Exposure effects on cardiac parameters

Analysis of heart rate across all treatment groups revealed no statistically significant effects of pollutant exposure (Table 4). The BaA + PS mixture was the only treatment that produced an elevated heart rate (23%) relative to the solvent control; however, this increase was not statistically significant. Similarly, stroke volume showed no statistically significant differences among treatments (Table 4), although larvae exposed to the All PCBs mixture exhibited a notable (non-significant) 63% increase in stroke volume.

Reductions in cardiac flow activity were observed exclusively in treatments involving single PCBs or PCB + PS mixtures (Table 4). Specifically, PCB 18 and PCB 18 + PS (significant for PCB 18 + PS only), PCB 81 + PS, PCB 105, and PCB 105 + PS all produced approximately 50% decreases in arterial flow activity relative to the solvent control. PCB 81 alone caused an even greater reduction, with a 79% decrease in flow activity. Although not statistically significant, larvae exposed to the All PCBs mixture exhibited a pronounced 90% reduction in cardiac flow

Table 3
EROD (in vivo) activity and mass-specific metabolic rate (MO_2) of zebrafish (n = 10 per treatment) exposed to single compounds and/or mixture treatments of a) PAHs (+PS), b) PCBs (+PS), and c) combined PAHs, PCBs, and PS. Asterisks (*p < 0.05, **p < 0.01, ***p < 0.001) indicate significant differences from the solvent control, whereas different letters denote significant differences among treatment groups with and without PS.

Treatments	EROD (μM/mg/h)		MO_2 (μg O_2/mg/h)	
	Without PS	With PS	Without PS	With PS
PAHs				
Solvent control	0.99	0.84	2.65 ± 0.35	2.34 ± 0.52
PHE	2.42	2.29	7.35 ± 1.16**	13.46 ± 4.16
PYR	1.20	0.74	5.54 ± 1.58	2.16 ± 0.52
BaA	0.90	0.96	3.03 ± 0.78	5.32 ± 1.92
IcdP	1.16	1.07	2.64 ± 0.40	2.54 ± 0.41
PCBs				
Solvent control	0.61		2.06 ± 0.28	
PCB 18	0.47	0.48	1.49 ± 0.20	0.89 ± 0.33
PCB 81	0.61	1.25	0.86 ± 0.20	4.40 ± 1.08
PCB 105	0.47	0.72	1.21 ± 0.25	1.46 ± 0.29
All PAHs/PCBs				
Solvent control	1.36		5.24 ± 0.65	
All PAHs	2.63	2.82	8.24 ± 0.94	4.35 ± 0.94
All PCBs	6.78	2.41	21.84 ± 3.83*** a	11.65 ± 3.91 b

activity (Table 4).

3.6. Multivariate principal component analysis (PCA) of exposure effects

The PCA biplot revealed a clear separation of treatments and their effects on sub-lethal endpoints (Fig. 2). Using a correlation matrix, the first two principal components accounted for 41.4% (PC1) and 25.4% (PC2) of the standardized variation across traits. Treatments involving single PCBs and PCB + PS mixtures clustered along PC2 and were most closely aligned with morphological endpoints such as body weight and length, indicating that PCB exposures primarily influenced morphology. In contrast, single PAHs and PAHs + PS mixtures aligned along PC1 and correlated with cardiac performance metrics such as heart rate, stroke volume, and flow activity, indicating that PAHs exposures exerted dominant effects on cardiovascular function.

Mixture treatments containing All PAHs and All PCBs were strongly associated together (along PC1) and showed a strong correspondence with metabolic endpoints, specifically mass-specific oxygen consumption rate (MO_2) and EROD activity. Similarly, MO_2 and EROD exhibited a strong positive and statistically significant correlation (Fig. 3; Pearson's $r = 0.9289$, $R^2 \approx 0.94$, $p < 0.0001$). This result indicates a close correspondence between CYP1A1-mediated monooxygenase induction (indexed by EROD activity) and whole-organism metabolic demand, with mixture exposures eliciting pronounced metabolic activation.

4. Discussion

In this study, the sub-lethal effects of single and mixture exposures of PAHs, PCBs, and polystyrene (PS) nanoplastics on larval zebrafish were examined. The selected PAHs and PCBs reflect the most abundant and environmentally relevant contaminants detected in fish collected from Matagorda Bay (Texas, USA). Consistent with previous research, exposure to both PAHs and PCBs (individually or as mixtures) produced adverse effects on metabolic and cardiac function (Incardona et al., 2004, 2006; Singleman and Holtzman, 2021; Green et al., 2025). The sub-lethal toxicity of PS nanoplastics was evaluated both alone and in combination with PAHs and PCBs. PS exposure alone did not significantly alter any measured physiological endpoints. However, co-exposure with either PHE or PCB 81 elevated MO_2 by 70% and 57%, respectively, suggesting that nanoplastics may modulate the metabolic consequences of contaminant exposure. Additionally, significant reductions in cardiac blood flow were observed in larvae co-exposed to PCB 18 + PS, PCB 81 + PS, and PCB 105 + PS. These findings suggest that the observed reductions in cardiovascular performance were specifically associated with PS co-exposure in the presence of PCBs, indicating that nanoplastics may also modulate PCB-induced toxicity rather than acting independently.

The mechanistic basis for these effects likely involves activation of the aryl hydrocarbon receptor (AhR) and subsequent induction of cytochrome P450 enzymes through the cytochrome P450 (CYP450) mixed-function monooxygenase system (Safe et al., 1985; Moorthy et al., 2015). This pathway is specific to planar aromatic contaminants such as PAHs and PCBs; polystyrene nanoplastics are not AhR ligands, and their contribution to the observed effects must therefore arise through a different mechanism. Induction of CYP1A1, a key isoform within this enzyme family, is regulated by the aryl hydrocarbon receptor (AhR) signaling pathway (Lo and Matthews, 2012). Both AhR and CYP450 systems are highly conserved (or shared) among invertebrate and vertebrate taxa (Beischlag et al., 2008) and activation of AhR by planar aromatic compounds is a central mechanism underlying their biological effects (Safe et al., 1985; Denison et al., 2002). Upon activation, AhR upregulates detoxification genes, including those encoding CYP450 enzymes (Rowlands et al., 1996; Beischlag et al., 2008).

Table 4
Heart rate, stroke volume, and blood-flow activity of zebrafish (n = 5 per treatment) exposed to single compounds and/or mixture treatments of a) PAHs (+PS), b) PCBs (+PS), and c) combined PAHs, PCBs, and PS. Asterisks (*p < 0.05, **p < 0.01, ***p < 0.001) indicate significant differences from the solvent control.

Treatment	Heart rate (beats/min)		Stroke vol (μl)		Flow activity (%)	
	Without PS	With PS	Without PS	With PS	Without PS	With PS
PAHs						
Solvent control	129.36 ± 11.75	117.07 ± 12.69	0.05 ± 0.01	0.05 ± 0.02	10.91 ± 1.65	11.66 ± 0.23
PHE	126.74 ± 11.67	128.44 ± 13.53	0.05 ± 0.01	0.04 ± 0.02	9.45 ± 1.79	4.47 ± 1.82
PYR	137.40 ± 9.63	143.55 ± 5.59	0.03 ± 0.00	0.05 ± 0.01	8.12 ± 0.69	9.43 ± 1.57
BaA	140.63 ± 4.61	162.16 ± 2.72	0.03 ± 0.01	0.06 ± 0.02	10.75	15.77 ± 1.21
IcdP	155.27 ± 4.86	151.76 ± 3.07	0.05 ± 0.01	0.04 ± 0.01	7.43 ± 1.53	12.41 ± 1.53
PCBs						
Solvent control	96.86 ± 13.07		0.03 ± 0.00		11.63 ± 1.52	
PCB 18	115.58 ± 9.11	97.56 ± 22.33	0.04 ± 0.02	0.01 ± 0.00	10.63 ± 0.86	5.82 ± 1.43*
PCB 81	128.50 ± 11.38	118.13 ± 13.64	0.02 ± 0.01	0.02 ± 0.01	2.48 ± 0.88***	5.48 ± 0.71*
PCB 105	97.38 ± 17.45	104.30 ± 20.51	0.03 ± 0.01	0.01 ± 0.00	7.72 ± 0.75	5.40 ± 0.83*
All PAHs/PCBs						
Solvent control	127.88 ± 1.95		0.02 ± 0.01		5.52 ± 1.26	
All PAHs	110.74 ± 7.10	137.55 ± 3.54	0.02 ± 0.01	0.02 ± 0.00	5.71 ± 1.75	5.60 ± 0.75
All PCBs	120.41 ± 6.94	114.26 ± 17.07	0.05 ± 0.01	0.03 ± 0.01	2.88 ± 0.91	5.09 ± 0.36

Aberrant AhR signaling and excessive CYP1A1 induction under PAH and PCB exposure are widely recognized drivers of developmental, metabolic, and cardiac toxicity (Incardona et al., 2004, 2014; Cherr et al., 2017; Takeshita et al., 2021). These adverse outcomes are thought to arise from CYP1A1 catalytic uncoupling, which disrupts electron transfer during monooxygenation reactions. This uncoupling generates reactive oxygen species, leading to oxidative stress and downstream cellular damage, including organelle disruption and DNA strand breaks (Wassenberg and Di Giulio, 2004; Green et al., 2008).

The mechanism by which PS nanoplastics modulate PCB-induced toxicity is likely indirect, operating through their physicochemical interaction with co-occurring contaminants rather than through AhR signaling. Owing to their high surface area and hydrophobicity, nanoplastics can sorb hydrophobic organic contaminants such as PCBs and PAHs, altering their bioavailability and acting as a vector that facilitates particle-associated uptake across biological membranes (Velzeboer et al., 2014; Koelmans et al., 2016). Once internalized, nanoplastics may also enhance contaminant toxicity through independent particle-level effects, including the generation of reactive oxygen species, membrane destabilization, and mitochondrial dysfunction, which can compound the oxidative stress already produced by CYP1A1 uncoupling (Brun et al., 2019; Bhagat et al., 2020). Together, these processes provide a plausible basis for the enhanced metabolic and cardiovascular responses observed under PCB + PS co-exposure, whereby the nanoplastic increases the effective internal dose and oxidative burden of the co-contaminant without itself activating the AhR pathway.

4.1. Exposure effects on morphometric parameters

The developmental toxicity of the selected contaminants was clearly evidenced by significant alterations to key morphometric parameters, including body weight, ocular and craniofacial area. The most severe outcomes were observed in the complex mixture groups. The complete mortality observed in the All PAHs + PCBs and All PAHs + PCBs + PS groups indicates an increased combined toxicity (although no significant Bliss interation), despite the individual contaminant concentrations being lower than acute toxicity thresholds (Billiard et al., 2006). Sublethal toxicity data was not acquired for groups with complete mortality (Fig. 1c). The stunted craniofacial development in the high mortality groups could be indicators of systemic developmental disruption (Raghunath and Perumal, 2018; Liu et al., 2020).

Individual PCBs (with or without PS) and particularly the dioxin-like PCB 81, were the largest driver of correlation observed in morphological data such as length and weight (Fig. 2). For example, exposures to PCB 81, All PCBs, and the complex All PAHs + PCBs mixtures, were consistently associated with the stunted craniofacial development (Fig. 1). This is consistent with the known potency of PCB 81 as a high-affinity ligand (Kd ≈ 5 nM) for the AhR (Hestermann et al., 2000). AhR activation drives the transcription of genes such as CYP1A, which can generate reactive oxygen species and disrupt normal signaling pathways critical for cardiovascular and craniofacial development; additionally, AhR-mediated interference with VEGF signaling has been implicated in the vascular defects and edema observed in zebrafish embryos (Incardona et al., 2004, 2011; Billiard et al., 2006). The significant 43% decrease in body weight in the PCB 81 + PS group, likely reflects developmental effects, underscoring its toxicity (Şişman et al., 2007; Singleman et al., 2021) (Table 3).

The role of PS nanoplastics appeared to be complex, modulating the toxicity of co-exposed chemicals in a manner that was not uniform. Our finding that the BaA + PS group exhibited a significant decrease in total length compared to controls suggest that PS co-exposure contributed to BaA's toxicity for this endpoint, although no significant Bliss interaction was observed (Sim et al., 2023; Tumwesigye et al., 2023). However, the co-exposure with PS did not lead to straightforward additive or synergistic toxicity. For instance, while the All PCBs group showed significant decrease in weight, the presence of PS showed no significant difference from the control group (Table 3). This suggests that the nanoplastics modify pollutant availability, potentially through competitive adsorption (due to affinity) among multiple contaminants on the plastic surface (Bakir et al., 2012). The sorption of chemicals to plastics can, in some cases, also reduce the freely available fraction in the water, potentially ameliorating the effects of exposure (Heinrich and Braunbeck, 2019; Sørensen et al., 2020). In a study conducted by Wang et al. (2022), zebrafish exposed to 100 μg/L PVC-MPs or 71 μg/L Di(2-ethylhexyl) phthalate (6 hpf to 9 dpf exposure) showed strong developmental, oxidative, and cardiac toxicity under single-pollutant conditions, but the combined microplastics exposure consistently produced lower toxicity (across hatching success, mortality, ROS production, and heart development) than either chemical alone. This antagonistic effect is due to PVC-MPs adsorbing Di(2-ethylhexyl) phthalate, thus reducing its bioavailability (Wang et al., 2022). Similarly, Coffin et al. (2020) showed BaP alone to significantly induce CYP1A (EROD) activity and impair phototaxis in juvenile white seabass (*Atractoscion nobilis*), while BaP-sorbed to polystyrene microplastics produced no measurable effects on enzyme activity or movement after 5 days of exposure. This indicates that the BaP sorbed onto plastics was less bioavailable than the freely dissolved BaP (Coffin et al., 2020).

4.2. Exposure effects on EROD activity and metabolic rate (MO_2)

The strong correlation between MO_2 and EROD activity suggests a functional linkage between metabolic rate and CYP1A-mediated biotransformation (Fig. 3). As described earlier, CYP450 enzymes catalyze mono-oxygenation reactions in which one atom of molecular oxygen (O_2) is incorporated into the substrate while the second atom is reduced to H_2O, a process that requires reducing equivalents such as NADPH (Miller, 2005; Guengerich, 2018). These oxidoreductase reactions are energetically demanding, and the catalytic activity of CYP450 enzymes is inherently dependent on the availability of molecular oxygen. The substantial catabolic power associated with CYP450-mediated oxidation (Jabłońska and Tawfik, 2022) therefore provides a mechanistic basis for the observed coupling between oxygen consumption and EROD activity. While the strong EROD–MO_2 correlation is consistent with CYP1A-linked oxygen demand, it may also reflect parallel induction of metabolic and detoxification pathways by AhR agonists. Thus, our data support co-induction rather than a direct causal relationship between CYP1A catalytic activity and whole-organism oxygen consumption.

This relationship is reflected in the PCA results (Fig. 2), where exposure to PAH and PCB mixtures (All PAHs and All PCBs) produced strong co-variation between EROD activity and MO_2. These findings indicate that in vivo EROD activity may serve as a useful proxy for oxygen consumption rate under conditions where pollutants share structural and mechanistic features. In particular, planar or co-planar polycyclic aromatic compounds such as PAHs and PCBs activate common pathways including AhR signaling and CYP450 induction, which can lead to additive or synergistic toxicological effects (Birnbaum and DeVito, 1995; Berg et al., 2006). Under such conditions, elevated CYP1A1 catalytic activity likely increases oxygen demand, thereby linking biotransformation capacity with whole-organism metabolic rate.

Overall, our study showed that exposure to the polystyrene (PS) nanoplastics alone did not induce any significant responses in the biomarkers measured. Rather co-exposure with contaminants showed modulatory effects, likely through the mechanism of kinetics, bioavailability and competitive pollutant sorption. For example, PHE alone caused a significant 46% increase in MO_2 relative to the solvent control, and this response was amplified, with the PHE + PS group showing a 70% increase in metabolic rate. Bliss analysis confirmed this as a significant synergistic interaction, the observed MO_2 of the PHE + PS group exceeding the predicted additive value (observed = 13.46 ± 4.16 vs. predicted = 7.59 μg O_2/mg/h; $\Delta = +5.87$, $p < 0.05$). This vector-mediated enhancement is consistent with a "Trojan horse" mechanism

(Trevisan et al., 2020), whereby sorption of a single hydrophobic contaminant onto PS increases its co-ingestion and internal delivery, raising the bioavailable dose above that of the freely dissolved compound (Bakir et al., 2012), and is supported by comparable findings in the literature such as the following. A study by Xu et al. (2021) found that adult zebrafish exposed for 12–24 days to 0.2 mg/L PHE together with 150 μm PS at 3 mg/L showed increased PHE accumulation, amplified oxidative-stress responses, heightened immune-gene activation, and greater gut-microbiome disruption compared with single-pollutant exposure (Xu et al., 2021). Ji et al. (2021) showed that polystyrene nanoplastics could act as efficient vectors for PAHs, with PS–BAP exposures (100 mg/kg PS + 2 mg/kg Bap) producing markedly higher cellular uptake and significantly stronger oxidative-stress and inflammatory responses than BAP alone at the same PAH dose (Ji et al., 2021).

In contrast, antagonistic effects emerged in the complex mixture. The All PCBs mixture caused a significant 84% increase in MO_2, yet co-exposure with PS (All PCBs + PS) resulted in a 47% decrease in MO_2 relative to the PCBs-only group (Table 4). Bliss analysis confirmed this reversal as a significant antagonistic interaction (observed $MO_2 = 11.65 \pm 3.91$ vs. predicted = 23.17 μg O_2/mg/h; $\Delta = -11.52$, $p < 0.05$), indicating that in complex mixtures PS reduced the bioavailability of certain congeners and exerted a protective effect (Sørensen et al., 2020; Martín et al., 2022). This contrast between the synergism of the isolated congener (PCB 81 + PS) and the antagonism of the full complex mixture can be explained by competitive sorption kinetics: because sorption affinity to PS scales with hydrophobicity (log Kow), the more hydrophobic congeners (PCB 81, log Kow = 6.42; PCB 105, ≈ 6.65) preferentially occupy the limited sorption sites when all congeners compete simultaneously, lowering the effective bioavailable fraction of the mixture as a whole (Llorca et al., 2020; Wang et al., 2020; Zhao et al., 2020). AhR pathway competition may further contribute, as the non-dioxin-like congener PCB 18 can dampen the AhR-mediated signal driven by the dioxin-like congeners, attenuating the collective metabolic response (Bakir et al., 2012).

The most pronounced toxicity was consistently associated with any treatment containing PCB 81, a potent dioxin-like congener (Giesy and Kannan, 1998). This dominance was borne out by the interaction analysis, in which PCB 81 + PS was the only PCB pairing to produce significant synergism for MO_2 (observed = 4.40 ± 1.08 vs. predicted = 0.48 μg O_2/mg/h; $\Delta = +3.92$, $p < 0.05$). Its influence likely explains the toxic response in the All PCBs mixture, which elicited the highest observed EROD induction (80% increase relative to the solvent control) and a statistically significant 84% elevation in metabolic rate as MO_2. The direct potency of this congener is evident, as the PCB 81 + PS exposure alone increased EROD activity by 51% and MO_2 by 57% (Table 4). As a non-ortho, coplanar molecule, PCB 81 is a potent agonist of the AhR, and activation of this pathway is a well-established mechanism for metabolic disruption and cardiotoxicity (Hestermann et al., 2000; Singleman and Holtzman, 2021). These results strongly indicate that the overall toxicity of the PCBs mixture was disproportionately driven by this single, high-potency congener. This is further supported by its toxic equivalency factor (TEF), which is 10× greater than that of PCB 105 (0.0003 for PCB 81 vs. 0.00003 for PCB 105) (Van den Berg et al., 2006), despite being present at half the concentration (0.002 μM for PCB 81 vs. 0.004 μM for PCB 105) in the treatment samples (Mortuza et al., 2025).

4.3. Exposure effects on cardiac parameters

Exposure to microplastics has been shown to induce cardiotoxic effects in fish (Persiani et al., 2023). A study by Sun et al. (2021) showed that embryo-larval zebrafish (up to 4 dph) exposed to 200 μg/L of 0.1 μm polyethylene (PE) nanoplastic beads exhibited increased pericardial edema and reduced blood flow, while heart rate remained unaffected. In their study, vascular endothelial damage led to vasodilation of blood vessels, which in turn decreased blood flow without altering cardiac rhythm (Sun et al., 2021). Similarly, in our study, reduced cardiac flow activity in several PCB + PS co-exposure groups, specifically PCB 18 + PS, PCB 81 + PS, and PCB 105 + PS were observed (Table 4). However, the concentration of plastics used here was 20-fold lower than that used by Sun et al. (2021). At an equivalent concentration to ours (10 μg/L), Sun et al. reported no detectable effects of PE microplastics on blood flow in embryo-larval zebrafish. This comparison strongly suggests that the reductions in cardiac flow observed in our PCB + PS treatments were primarily driven by PCB toxicity rather than by PS nanoplastics. This interpretation is further supported by the absence of any statistically significant effects on cardiac flow in the PS-only treatment group. Bliss Independence testing revealed that for PCB 81 + PS, the observed flow activity did not differ significantly from the additive prediction ($\Delta = +1.57\%$, $p > 0.05$); because PCB 81 alone already produced a significant reduction in flow activity, this confirms that PCB 81, rather than PS, was the primary driver, with PS providing no additional reduction. In a study conducted by Green et al. (2025), exposing zebrafish embryos to the PCBs mixture Aroclor 1254 caused concentration-dependent bradycardia, with heart rates decreasing as PCBs tissue levels increased. In addition, larvae exhibited a novel tremor behavior, highlighting both cardiac and neurological developmental toxicity (Green et al., 2025). PCBs are well-documented to accumulate in human tissues, and elevated PCB body burdens have been associated with hypertension and other vascular dysfunctions (Goncharov et al., 2011; Perkins et al., 2016). In the context of our study, it remains unclear whether the reduced cardiac blood flow observed in several PCB + PS treatment groups (Table 5) reflects early-stage vascular impairment that could later manifest as hypertension or altered vascular tone. Nonetheless, these findings highlight the value of incorporating cardiac morphology and functional endpoints into toxicity assessments. Such biomarkers may reveal conserved mechanisms of adverse effects shared across wildlife and humans exposed to persistent pollutants (PAHs, PCBs) and emerging contaminants such as NMPs.

The PCA analysis (Fig. 2) indicates that much of the correlation in cardiac performance (i.e., heart rate, stroke volume, and flow activity) is strongly associated with single treatment PAHs, such as for PHE, BaA and IcdP. This result agrees with findings from Incardona et al. (2004), who demonstrated that exposure of zebrafish embryos to specific PAHs, such as PHE and DBT (dibenzothiophene), induced severe cardiac dysfunction prior to the onset of morphological abnormalities (Incardona et al., 2004). Three-ring PAHs, such as PHE, primarily disrupt cardiac function by interfering with specific cardiac ion channels (potassium and calcium channels), leading to secondary developmental defects in organs and skeletal structures as well as edema from disruption in blood flow. Additionally, four and five-ring PAHs such as PYR and BaP (benzo[*a*]pyrene) utilize the AhR pathway, leading to the induction of CYP1A enzymes and subsequent toxic effects, which typically include anemia and peripheral vascular defects (Incardona et al., 2006, 2011). These findings indicate two distinct, and potentially interactive, mechanisms of toxicity in aquatic vertebrates. The first, a direct interference with cardiac ion channels, and the second involving AhR-mediated signaling that induces CYP1A activity and subsequent toxic effects. (Incardona et al., 2004, 2006, 2011). Therefore, our results indicate that PAHs exert a more direct and pronounced effect on cardiac performance, consistent with their role as potent cardio toxicants during early developmental life stages (Incardona et al., 2011; Incardona and Scholz, 2016; Cunha et al., 2020; Sim et al., 2023).

4.4. Implications for wildlife toxicity

The differential responses observed between chemical and NMP particulate contaminants likely reflect fundamental differences in mode of action. PAHs and PCBs are well-known ligands of the aryl hydrocarbon receptor (AHR) and elicit downstream CYP1A induction, increasing metabolic demand and contributing to cardiotoxicity (Willett et al., 1997; Nilsen et al., 1998; Incardona et al., 2004; Wassenberg and Di

Giulio, 2004; Green et al., 2008; Singleman and Holtzman, 2021). The strong correspondence between EROD activity and elevated MO_2 observed in this study underscores the energetic cost associated with CYP450-mediated biotransformation (Miller, 2005; Guengerich, 2018; Jabłońska and Tawfik, 2022). In contrast, NMPs lack known biological molecular initiating events (i.e., target receptors or enzymes), which may explain their comparatively low toxicity despite being orders of magnitude more abundant than PAHs and PCBs in aquatic biota (Mortuza et al., 2025). Conversely, NMPs associated toxicity may stem from particle accumulation within tissues and subsequent inflammatory responses (Li et al., 2020; Pirsaheb et al., 2020; Zhao et al., 2021; Mahmud et al., 2024). Moreover, plastics may serve as carriers for sorbed contaminants or release plastic additives such as plasticizers (with well understood toxicities), which can contribute to adverse health effects (Meeker et al., 2009; Bakir et al., 2012; Rochman et al., 2014b; Hahladakis et al., 2018; Campanale et al., 2020; Gardon et al., 2020; Herrera et al., 2022). Overall, we expect PAHs and PCBs body-burdens to be prominent drivers of sub-lethal toxicity in exposed aquatic biota. However, continued investigation of NMPs is warranted due to their ubiquity, potential additive effects in contaminant mixtures, and their capacity to transport sorbed chemicals or release plastic additives such as plasticizers. Given these considerations, reduction in the use of single-use plastics is recommended as a precautionary measure to limit environmental loading.

5. Conclusions

In this study, exposure of larval zebrafish to mixtures of PAHs or PCBs resulted in a pronounced induction of CYP450-mediated biotransformation activity, as reflected by elevated EROD responses. This increase in EROD activity coincided with higher metabolic (oxygen consumption) rates (MO_2), suggesting that the enhanced metabolic demand for molecular oxygen supports the co-induction of mono-oxygenation reactions catalyzed by CYP450 enzymes. In contrast, exposure to polystyrene (PS) nanoplastic particles alone did not produce significant changes in any of the measured biomarkers. However, when fish were co-exposed to PHE + PS or PCB 81 + PS, MO_2 levels increased by 70% and 57%, respectively, relative to the solvent control (0.1% DMSO), indicative of synergistic effects (according to Bliss Independence analysis). Additionally, a significant reduction in cardiac blood flow in larvae exposed to PCB 18, PCB 81, and PCB 105 in combination with PS was observed. This was attributed primarily to the PCB co-exposure with PS, as PS nanoplastics alone did not alter blood flow. Overall, our findings demonstrate that in vivo EROD activity serves as a useful proxy for MO_2-based assessments of PAH and PCB exposure and underscore the importance of incorporating multi-biomarker sublethal toxicity evaluations of both persistent pollutants (PAHs, PCBs) and emerging contaminants such as NMPs mixtures in environmentally relevant concentrations.

CRediT authorship contribution statement

Asif Mortuza: Writing – review & editing, Writing – original draft, Visualization, Software, Methodology, Investigation, Formal analysis, Data curation, Conceptualization. **Daniel Kemp:** Software, Methodology, Investigation, Data curation. **Antonietta Quigg:** Writing – review & editing, Supervision, Funding acquisition. **R.J. David Wells:** Writing – review & editing, Supervision, Funding acquisition. **Karl Kaiser:** Supervision, Funding acquisition, Conceptualization. **David Hala:** Writing – review & editing, Writing – original draft, Supervision, Resources, Project administration, Investigation, Funding acquisition, Formal analysis, Conceptualization. **Lene H. Petersen:** Writing – review & editing, Supervision, Software, Resources, Methodology, Funding acquisition, Conceptualization.

Ethics declaration

This study was conducted in accordance with the ARRIVE (Animal Research: Reporting of In Vivo Experiments) guidelines.

This study was approved by the Institutional Animal Care and Use Committee (IACUC) (Approval No. 2024-0013).

Declaration of competing interest

The authors declare that they have no known competing financial interests or personal relationships that could have appeared to influence the work reported in this paper.

Acknowledgements

This work was supported by the Matagorda Bay Mitigation Trust (Grant #013) awarded to Hala, Kaiser, Wells, Quigg, and Petersen. Additional funding was provided by the Texas Comptroller of Public Accounts (Grant #CMD 19-6799CS to Wells) and by the U.S. Army Corps of Engineers (Grant #ERDC BAA 21-0045A to Kaiser).

Appendix A. Supplementary data

Supplementary data to this article can be found online at https://doi.org/10.1016/j.cbpc.2026.110633.

Data availability

Data will be made available on request.

References

Andrady, A.L., 2011. Microplastics in the marine environment. Mar. Pollut. Bull. 62 (8), 1596–1605.

Assas, M., Qiu, X., Chen, K., Ogawa, H., Xu, H., Shimasaki, Y., Oshima, Y., 2020. Bioaccumulation and reproductive effects of fluorescent microplastics in medaka fish. Mar. Pollut. Bull. 158, 111446. https://doi.org/10.1016/j.marpolbul.2020.111446.

Bacosa, H.P., Steichen, J., Kamalanathan, M., Windham, R., Lubguban, A., Labonte, J.M., Kaiser, K., Hala, D., Santschi, P.H., Quigg, A., 2020. Polycyclic aromatic hydrocarbons (PAHs) and putative PAH-degrading bacteria in Galveston Bay, TX (USA), following Hurricane Harvey (2017). Environ. Sci. Pollut. Res. Int. 27 (28), 34987–34999. https://doi.org/10.1007/s11356-020-09754-5.

Bagatto, B., Pelster, B., Burggren, W., 2001. Growth and metabolism of larval zebrafish: effects of swim training. J. Exp. Biol. 204 (24), 4335–4343.

Bakir, A., Rowland, S.J., Thompson, R.C., 2012. Competitive sorption of persistent organic pollutants onto microplastics in the marine environment. Mar. Pollut. Bull. 64 (12), 2782–2789. https://doi.org/10.1016/j.marpolbul.2012.09.010.

Barboza, L.G.A., Vieira, L.R., Branco, V., Figueiredo, N., Carvalho, F., Carvalho, C., Guilhermino, L., 2018. Microplastics cause neurotoxicity, oxidative damage and energy-related changes and interact with the bioaccumulation of mercury in the European seabass, Dicentrarchus labrax (Linnaeus, 1758). Aquat. Toxicol. 195, 49–57.

Barrionuevo, W., Burggren, W., 1999. O2 consumption and heart rate in developing zebrafish (*Danio rerio*): influence of temperature and ambient O2. Am. J. Phys. Regul. Integr. Comp. Phys. 276 (2), R505–R513.

Barrionuevo, W., Fernandes, M., Rocha, O., 2010. Aerobic and anaerobic metabolism for the zebrafish, Danio rerio, reared under normoxic and hypoxic conditions and exposed to acute hypoxia during development. Braz. J. Biol. 70, 425–434.

Beischlag, T.V., Luis Morales, J., Hollingshead, B.D., Perdew, G.H., 2008. The aryl hydrocarbon receptor complex and the control of gene expression. Crit. Rev. Eukaryot. Gene Expr. 18 (3), 207–250.

Berg, M., Birnbaum, L., Denison, M., De, M., Farland, W., Feeley, M., Fiedler, H., Håkansson, H., Hanberg, A., Haws, L., Rose, M., Safe, S., Schrenk, D., Tohyama, C., Tritscher, A., Tuomisto, J., Tysklind, M., Walker, N., Peterson, R., 2006. Review the 2005 World Health Organization reevaluation of human and mammalian toxic equivalency factors for dioxins and dioxin-like compounds. Toxicol. Sci. 93, 223–241.

Bermúdez, J., Swarzenski, P., 2021. A microplastic size classification scheme aligned with universal plankton survey methods. MethodsX 8, 101516.

Bhagat, J., Zang, L., Nishimura, N., Shimada, Y., 2020. Zebrafish: an emerging model to study microplastic and nanoplastic toxicity. Sci. Total Environ. 728, 138707. https://doi.org/10.1016/j.scitotenv.2020.138707.

Billiard, S.M., Timme-Laragy, A.R., Wassenberg, D.M., Cockman, C., Di Giulio, R.T., 2006. The role of the aryl hydrocarbon receptor pathway in mediating synergistic

developmental toxicity of polycyclic aromatic hydrocarbons to zebrafish. Toxicol. Sci. 92 (2), 526–536. https://doi.org/10.1093/toxsci/kfl011.
Birnbaum, L.S., DeVito, M.J., 1995. Use of toxic equivalency factors for risk assessment for dioxins and related compounds. Toxicology 105 (2–3), 391–401. https://doi.org/10.1016/0300-483x(95)03237-a.
Black, J.A., Birge, W.J., Westerman, A.G., Francis, P.C., 1983. Comparative aquatic toxicology of aromatic hydrocarbons. Fundam. Appl. Toxicol. 3 (5), 353–358.
Bliss, C.I., 1939. The toxicity of poisons applied jointly. Ann. Appl. Biol. 26 (3), 585–615. https://doi.org/10.1111/j.1744-7348.1939.tb06990.x.
Boyle, R.H., Highland, J.H., 1979. The persistence of PCBs. Environ. Sci. Policy Sustain. Dev. 21 (5), 6–37.
Brandts, I., Teles, M., Gonçalves, A., Barreto, A., Franco-Martinez, L., Tvarijonaviciute, A., Martins, M., Soares, A., Tort, L., Oliveira, M., 2018. Effects of nanoplastics on *Mytilus galloprovincialis* after individual and combined exposure with carbamazepine. Sci. Total Environ. 643, 775–784.
Brennecke, D., Duarte, B., Paiva, F., Caçador, I., Canning-Clode, J., 2016. Microplastics as vector for heavy metal contamination from the marine environment. Estuar. Coast. Shelf Sci. 178, 189–195.
Brett, J.R., 1964. The respiratory metabolism and swimming performance of young sockeye salmon. J. Fish. Res. Board Can. 21 (5), 1183–1226.
Brun, N.R., van Hage, P., Hunting, E.R., Haramis, A.-P.G., Vink, S.C., Vijver, M.G., Schaaf, M.J.M., Tudorache, C., 2019. Polystyrene nanoplastics disrupt glucose metabolism and cortisol levels with a possible link to behavioural changes in larval zebrafish. Commun. Biol. 2 (1), 382. https://doi.org/10.1038/s42003-019-0629-6.
Bruss, Z.S., Raja, A., 2025. Physiology, stroke volume. In: StatPearls. StatPearls Publishing Copyright © 2025, StatPearls Publishing LLC.
Campanale, C., Massarelli, C., Savino, I., Locaputo, V., Uricchio, V.F., 2020. A detailed review study on potential effects of microplastics and additives of concern on human health. Int. J. Environ. Res. Public Health 17 (4), 1212.
Carpenter, D.O., 1998. Polychlorinated biphenyls and human health. Int. J. Occup. Med. Environ. Health 11 (4), 291–303.
Chamas, A., Moon, H., Zheng, J., Qiu, Y., Tabassum, T., Jang, J.H., Abu-Omar, M., Scott, S.L., Suh, S., 2020. Degradation rates of plastics in the environment. ACS Sustain. Chem. Eng. 8 (9), 3494–3511.
Cherr, G.N., Fairbairn, E.A., Whitehead, A., 2017. Impacts of petroleum-derived pollutants on fish development. Annu. Rev. Anim. Biosci. 5, 185–203.
Coffin, S., Magnuson, J.T., Vliet, S.M., Volz, D.C., Schlenk, D., 2020. Effects of short-term exposure to environmentally-relevant concentrations of benzo (a) pyrene-sorbed polystyrene to white seabass (*Atractoscion nobilis*). Environ. Pollut. 263, 114617.
Cunha, V., Vogs, C., Le Bihanic, F., Dreij, K., 2020. Mixture effects of oxygenated PAHs and benzo[a]pyrene on cardiovascular development and function in zebrafish embryos. Environ. Int. 143, 105913. https://doi.org/10.1016/j.envint.2020.105913.
Dawson, A., Huston, W., Kawaguchi, S., King, C., Cropp, R., Wild, S., Eisenmann, P., Townsend, K., Bengtson Nash, S., 2018. Uptake and depuration kinetics influence microplastic bioaccumulation and toxicity in Antarctic krill (Euphausia superba). Environ. Sci. Technol. 52 (5), 3195–3201.
Deng, Y., Zhang, Y., Lemos, B., Ren, H., 2017. Tissue accumulation of microplastics in mice and biomarker responses suggest widespread health risks of exposure. Sci. Rep. 7 (1), 1–10.
Denison, M.S., Pandini, A., Nagy, S.R., Baldwin, E.P., Bonati, L., 2002. Ligand binding and activation of the Ah receptor [Research Support, Non-U S Gov't Research Support, U S Gov't, P H S Review]. Chem. Biol. Interact. 141 (1–2), 3–24.
Ding, J., Zhang, S., Razanajatovo, R.M., Zou, H., Zhu, W., 2018. Accumulation, tissue distribution, and biochemical effects of polystyrene microplastics in the freshwater fish red tilapia (Oreochromis niloticus). Environ. Pollut. 238, 1–9.
Donkers, J.M., Höppener, E.M., Grigoriev, I., Will, L., Melgert, B.N., van der Zaan, B., van de Steeg, E., Kooter, I.M., 2022. Advanced epithelial lung and gut barrier models demonstrate passage of microplastic particles. Microplastics Nanoplastics 2 (1), 6.
Eisler, R., Belisle, A.A., 1996. Planar PCB Hazards to Fish, Wildlife, and Invertebrates: A Synoptic Review. US Department of the Interior, National Biological Service.
Fry, F., 1971. The effect of environmental factors on the physiology of fish. In: Fish Physiology, vol. 6. Elsevier, pp. 1–98.
Gahn, M.B., Wharton, M., Mortuza, A., Hala, D., Marshall, C.D., Kaiser, K., 2025. Rapid and sensitive quantification of nano- and microplastics in water, sediment, and biological tissue by pyrolysis-gas chromatography tandem mass spectrometry with dynamic reaction monitoring. Anal. Chem. https://doi.org/10.1021/acs.analchem.5c05604.
Gall, S.C., Thompson, R.C., 2015. The impact of debris on marine life. Mar. Pollut. Bull. 92 (1–2), 170–179.
Garcès, A., Soeiro, V., Loio, S., Pires, I., 2024. Mortality from plastic ingestion and net entanglement in marine birds–description of three cases. Vet. Glas. 78 (2), 190–196.
Gardon, T., Huvet, A., Paul-Pont, I., Cassone, A.-L., Sham Koua, M., Soyez, C., Jezequel, R., Receveur, J., Le Moullac, G., 2020. Toxic effects of leachates from plastic pearl-farming gear on embryo-larval development in the pearl oyster Pinctada margaritifera. Water Res. 179, 115890. https://doi.org/10.1016/j.watres.2020.115890.
Giesy, J.P., Kannan, K., 1998. Dioxin-like and non-dioxin-like toxic effects of polychlorinated biphenyls (PCBs): implications for risk assessment. Crit. Rev. Toxicol. 28 (6), 511–569.
Goncharov, A., Pavuk, M., Foushee, H.R., Carpenter, D.O., 2011. Blood pressure in relation to concentrations of PCB congeners and chlorinated pesticides. Environ. Health Perspect. 119 (3), 319–325. https://doi.org/10.1289/ehp.1002830.
Green, R.M., Hodges, N.J., Chipman, J.K., O'Donovan, M.R., Graham, M., 2008. Reactive oxygen species from the uncoupling of human cytochrome P450 1B1 may contribute to the carcinogenicity of dioxin-like polychlorinated biphenyls. Mutagenesis 23 (6), 457–463. https://doi.org/10.1093/mutage/gen035.
Green, C.S., Morris, J.M., Magnuson, J.T., Leads, R.R., Lay, C.R., Gielazyn, M., Rosman, L., Schlenk, D., Roberts, A.P., 2025. Exposure to the polychlorinated biphenyl mixture Aroclor 1254 elicits neurological and cardiac developmental effects in early life stage zebrafish (Danio rerio). Chemosphere 371, 144023. https://doi.org/10.1016/j.chemosphere.2024.144023.
Gregory, M.R., 2009. Environmental implications of plastic debris in marine settings—entanglement, ingestion, smothering, hangers-on, hitch-hiking and alien invasions. Philos. Trans. R. Soc. Lond. Ser. B Biol. Sci. 364 (1526), 2013–2025. https://doi.org/10.1098/rstb.2008.0265.
Guengerich, F.P., 2018. Mechanisms of cytochrome P450-catalyzed oxidations. ACS Catal. 8 (12), 10964–10976. https://doi.org/10.1021/acscatal.8b03401.
Guo, X., Lv, M., Li, J., Ding, J., Wang, Y., Fu, L., Sun, X., Han, X., Chen, L., 2022. The distinct toxicity effects between commercial and realistic polystyrene microplastics on microbiome and histopathology of gut in zebrafish. J. Hazard. Mater. 434, 128874. https://doi.org/10.1016/j.jhazmat.2022.128874.
Hahladakis, J.N., Velis, C.A., Weber, R., Iacovidou, E., Purnell, P., 2018. An overview of chemical additives present in plastics: migration, release, fate and environmental impact during their use, disposal and recycling. J. Hazard. Mater. 344, 179–199.
Hamers, T., Kamstra, J.H., Cenijn, P.H., Pencikova, K., Palkova, L., Simeckova, P., Vondracek, J., Andersson, P.L., Stenberg, M., Machala, M., 2011. In vitro toxicity profiling of ultrapure non–dioxin-like polychlorinated biphenyl congeners and their relative toxic contribution to PCB mixtures in humans. Toxicol. Sci. 121 (1), 88–100.
Heinrich, P., Braunbeck, T., 2019. Bioavailability of microplastic-bound pollutants in vitro: the role of adsorbate lipophilicity and surfactants. Comp. Biochem. Physiol. C Toxicol. Pharmacol. 221, 59–67. https://doi.org/10.1016/j.cbpc.2019.03.012.
Herrera, A., Acosta-Dacal, A., Pérez Luzardo, O., Martínez, I., Rapp, J., Reinold, S., Montesdeoca-Esponda, S., Montero, D., Gómez, M., 2022. Bioaccumulation of additives and chemical contaminants from environmental microplastics in European seabass (Dicentrarchus labrax). Sci. Total Environ. 822, 153396. https://doi.org/10.1016/j.scitotenv.2022.153396.
Hestermann, E.V., Stegeman, J.J., Hahn, M.E., 2000. Relative contributions of affinity and intrinsic efficacy to aryl hydrocarbon receptor ligand potency. Toxicol. Appl. Pharmacol. 168 (2), 160–172. https://doi.org/10.1006/taap.2000.9026.
Hoage, T., Ding, Y., Xu, X., 2012. Quantifying cardiac functions in embryonic and adult zebrafish. In: Cardiovascular Development: Methods and Protocols, pp. 11–20.
Honda, M., Suzuki, N., 2020. Toxicities of polycyclic aromatic hydrocarbons for aquatic animals. Int. J. Environ. Res. Public Health 17 (4). https://doi.org/10.3390/ijerph17041363.
Howell, N.L., Lakshmanan, D., Rifai, H.S., Koenig, L., 2011. PCB dry and wet weather concentration and load comparisons in Houston-area urban channels. Sci. Total Environ. 409 (10), 1867–1888.
Hu, N., Yost, H.J., Clark, E.B., 2001. Cardiac morphology and blood pressure in the adult zebrafish. Anat. Rec. 264 (1), 1–12.
Hu, C.J., Garcia, M.A., Nihart, A., Liu, R., Yin, L., Adolphi, N., Gallego, D.F., Kang, H., Campen, M.J., Yu, X., 2024a. Microplastic presence in dog and human testis and its potential association with sperm count and weights of testis and epididymis. Toxicol. Sci., kfae060 https://doi.org/10.1093/toxsci/kfae060.
Hu, Y., Nie, F., Zhang, M., Song, Q., Wei, W., Lv, G., Wei, Y., Kang, D., Chen, Z., Lin, H., Chen, J., 2024b. Developmental toxicity and mechanism of polychlorinated biphenyls 126 and nano-polystyrene combined exposure to zebrafish larvae. Ecotoxicol. Environ. Saf. 278, 116419. https://doi.org/10.1016/j.ecoenv.2024.116419.
Incardona, J.P., Scholz, N.L., 2016. The influence of heart developmental anatomy on cardiotoxicity-based adverse outcome pathways in fish. Aquat. Toxicol. 177, 515–525. https://doi.org/10.1016/j.aquatox.2016.06.016.
Incardona, J.P., Collier, T.K., Scholz, N.L., 2004. Defects in cardiac function precede morphological abnormalities in fish embryos exposed to polycyclic aromatic hydrocarbons. Toxicol. Appl. Pharmacol. 196 (2), 191–205. https://doi.org/10.1016/j.taap.2003.11.026.
Incardona, J.P., Day, H.L., Collier, T.K., Scholz, N.L., 2006. Developmental toxicity of 4-ring polycyclic aromatic hydrocarbons in zebrafish is differentially dependent on AH receptor isoforms and hepatic cytochrome P4501A metabolism. Toxicol. Appl. Pharmacol. 217 (3), 308–321. https://doi.org/10.1016/j.taap.2006.09.018.
Incardona, J.P., Linbo, T.L., Scholz, N.L., 2011. Cardiac toxicity of 5-ring polycyclic aromatic hydrocarbons is differentially dependent on the aryl hydrocarbon receptor 2 isoform during zebrafish development. Toxicol. Appl. Pharmacol. 257 (2), 242–249. https://doi.org/10.1016/j.taap.2011.09.010.
Incardona, J.P., Gardner, L.D., Linbo, T.L., Brown, T.L., Esbaugh, A.J., Mager, E.M., Stieglitz, J.D., French, B.L., Labenia, J.S., Laetz, C.A., Tagal, M., Sloan, C.A., Elizur, A., Benetti, D.D., Grosell, M., Block, B.A., Scholz, N.L., 2014. Deepwater Horizon crude oil impacts the developing hearts of large predatory pelagic fish. Proc. Natl. Acad. Sci. USA 111 (15), E1510–E1518. https://doi.org/10.1073/pnas.1320950111.
Jabłońska, J., Tawfik, D.S., 2022. Innovation and tinkering in the evolution of oxidases. Protein Sci. 31 (5), e4310. https://doi.org/10.1002/pro.4310.
Jeong, E., Lee, J.-Y., Redwan, M., 2024. Animal exposure to microplastics and health effects: a review. Emerg. Contam. 10 (4), 100369. https://doi.org/10.1016/j.emcon.2024.100369.
Ji, Y., Wang, Y., Shen, D., Kang, Q., Chen, L., 2021. Mucin corona delays intracellular trafficking and alleviates cytotoxicity of nanoplastic-benzopyrene combined contaminant. J. Hazard. Mater. 406, 124306. https://doi.org/10.1016/j.jhazmat.2020.124306.

Kannan, K., Vimalkumar, K., 2021. A review of human exposure to microplastics and insights into microplastics as obesogens [review]. Front. Endocrinol. 12. https://doi.org/10.3389/fendo.2021.724989.
Kenyon, K.W., Kridler, E., 1969. Laysan albatrosses swallow indigestible matter. Auk 86 (2), 339–343.
Knecht, A.L., Goodale, B.C., Truong, L., Simonich, M.T., Swanson, A.J., Matzke, M.M., Anderson, K.A., Waters, K.M., Tanguay, R.L., 2013. Comparative developmental toxicity of environmentally relevant oxygenated PAHs. Toxicol. Appl. Pharmacol. 271 (2), 266–275.
Koelmans, A.A., Bakir, A., Burton, G.A., Janssen, C.R., 2016. Microplastic as a vector for chemicals in the aquatic environment: critical review and model-supported reinterpretation of empirical studies. Environ. Sci. Technol. 50 (7), 3315–3326. https://doi.org/10.1021/acs.est.5b06069.
Lakshmanan, D., Howell, N.L., Rifai, H.S., Koenig, L., 2010. Spatial and temporal variation of polychlorinated biphenyls in the Houston Ship Channel. Chemosphere 80 (2), 100–112.
Lapointe, D., Vogelbein, W.K., Fabrizio, M.C., Gauthier, D.T., Brill, R.W., 2014. Temperature, hypoxia, and mycobacteriosis: effects on adult striped bass Morone saxatilis metabolic performance. Dis. Aquat. Org. 108 (2), 113–127.
LeMoine, C.M., Kelleher, B.M., Lagarde, R., Northam, C., Elebute, O.O., Cassone, B.J., 2018. Transcriptional effects of polyethylene microplastics ingestion in developing zebrafish (*Danio rerio*). Environ. Pollut. 243, 591–600.
Leslie, H.A., van Velzen, M.J.M., Brandsma, S.H., Vethaak, A.D., Garcia-Vallejo, J.J., Lamoree, M.H., 2022. Discovery and quantification of plastic particle pollution in human blood. Environ. Int. 163, 107199. https://doi.org/10.1016/j.envint.2022.107199.
Li, B., Ding, Y., Cheng, X., Sheng, D., Xu, Z., Rong, Q., Wu, Y., Zhao, H., Ji, X., Zhang, Y., 2020. Polyethylene microplastics affect the distribution of gut microbiota and inflammation development in mice. Chemosphere 244, 125492.
Li, Y., Tao, L., Wang, Q., Wang, F., Li, G., Song, M., 2023. Potential health impact of microplastics: a review of environmental distribution, human exposure, and toxic effects. Environ. Health 1 (4), 249.
Liu, Z., Yu, P., Cai, M., Wu, D., Zhang, M., Huang, Y., Zhao, Y., 2019. Polystyrene nanoplastic exposure induces immobilization, reproduction, and stress defense in the freshwater cladoceran Daphnia pulex. Chemosphere 215, 74–81.
Liu, S., Narumi, R., Ikeda, N., Morita, O., Tasaki, J., 2020. Chemical-induced craniofacial anomalies caused by disruption of neural crest cell development in a zebrafish model. Dev. Dyn. 249 (7), 794–815. https://doi.org/10.1002/dvdy.179.
Llorca, M., Ábalos, M., Vega-Herrera, A., Adrados, M.A., Abad, E., Farré, M., 2020. Adsorption and desorption behaviour of polychlorinated biphenyls onto microplastics' surfaces in water/sediment systems. Toxics 8 (3), 59.
Lo, R., Matthews, J., 2012. High-resolution genome-wide mapping of AHR and ARNT binding sites by ChIP-Seq [Research Support, Non-U S Gov't]. Toxicol. Sci. 130 (2), 349–361.
Mahmud, F., Sarker, D.B., Jocelyn, J.A., Sang, Q.X.A., 2024. Molecular and cellular effects of microplastics and nanoplastics: focus on inflammation and senescence. Cells 13 (21), 1788.
Martín, J., Santos, J.L., Aparicio, I., Alonso, E., 2022. Microplastics and associated emerging contaminants in the environment: analysis, sorption mechanisms and effects of co-exposure. Trends Environ. Anal. Chem. 35, e00170. https://doi.org/10.1016/j.teac.2022.e00170.
Meeker, J.D., Sathyanarayana, S., Swan, S.H., 2009. Phthalates and other additives in plastics: human exposure and associated health outcomes. Philos. Trans. R. Soc. B Biol. Sci. 364 (1526), 2097–2113.
Miller, W.L., 2005. Minireview: regulation of steroidogenesis by electron transfer. Endocrinology 146 (6), 2544–2550. https://doi.org/10.1210/en.2005-0096.
Monosson, E., 2000. Reproductive and developmental effects of PCBs in fish: a synthesis of laboratory and field studies. Rev. Toxicol. 3 (1), 25–75.
Moorthy, B., Chu, C., Carlin, D.J., 2015. Polycyclic aromatic hydrocarbons: from metabolism to lung cancer [Research Support, N I H, Extramural Review]. Toxicol. Sci. 145 (1), 5–15.
Mortuza, Meese, E.N., Wharton, M., Gahn, B., Petersen, L.H., Quigg, A., Wells, R.J.D., Kaiser, K., Hala, D., 2025. Comparing persistent (polycyclic aromatic hydrocarbons and polychlorinated biphenyls) and emerging nano(micro)plastics (NMPs) pollutant body-burdens in oysters and fish from Matagorda Bay (Texas, USA). Mar. Pollut. Bull. 221, 118495. https://doi.org/10.1016/j.marpolbul.2025.118495.
Naderi, A.M., Casey, J.G., Huang, M.-H., Victorio, R., Chiang, D.Y., MacRae, C., Cao, H., Gupta, V.A., 2024. Towards precision cardiovascular analysis in zebrafish: the ZACAF paradigm. arXiv preprint. arXiv:2402.09658.
Nihart, A.J., Garcia, M.A., El Hayek, E., Liu, R., Olewine, M., Kingston, J.D., Castillo, E.F., Gullapalli, R.R., Howard, T., Bleske, B., 2025. Bioaccumulation of microplastics in decedent human brains. Nat. Med. 31 (4), 1114–1119.
Nilsen, B.M., Berg, K., Goksøyr, A., 1998. Induction of cytochrome P450 1A (CYP1A) in fish. A biomarker for environmental pollution. Methods Mol. Biol. 107, 423–438. https://doi.org/10.1385/0-89603-519-0:423.
Noldus, 2025. DanioScope Resources. https://noldus.com/danioscope/resources.
Noury, P., Geffard, O., Tutundjian, R., Garric, J., 2006. Non destructive in vivo measurement of ethoxyresorufin biotransformation by zebrafish prolarva: development and application. Environ. Toxicol. 21 (4), 324–331.
Perkins, J.T., Petriello, M.C., Newsome, B.J., Hennig, B., 2016. Polychlorinated biphenyls and links to cardiovascular disease. Environ. Sci. Pollut. Res. Int. 23 (3), 2160–2172. https://doi.org/10.1007/s11356-015-4479-6.
Persiani, E., Cecchettini, A., Ceccherini, E., Gisone, I., Morales, M.A., Vozzi, F., 2023. Microplastics: a matter of the heart (and vascular system). Biomedicines 11 (2). https://doi.org/10.3390/biomedicines11020264.
Petersen, L., Gamperl, A., 2010. Effect of acute and chronic hypoxia on the swimming performance, metabolic capacity and cardiac function of Atlantic cod (*Gadus morhua*). J. Exp. Biol. 213 (5), 808–819.
Pettersen, A.K., White, C.R., Marshall, D.J., 2016. Metabolic rate covaries with fitness and the pace of the life history in the field. Proc. R. Soc. B Biol. Sci. 283 (1831), 20160323.
Pettersen, A.K., Marshall, D.J., White, C.R., 2018. Understanding variation in metabolic rate. J. Exp. Biol. 221 (1), jeb166876.
Pirsaheb, M., Hossini, H., Makhdoumi, P., 2020. Review of microplastic occurrence and toxicological effects in marine environment: experimental evidence of inflammation. Process. Saf. Environ. Prot. 142, 1–14.
Pitt, J.A., Trevisan, R., Massarsky, A., Kozal, J.S., Levin, E.D., Di Giulio, R.T., 2018. Maternal transfer of nanoplastics to offspring in zebrafish (Danio rerio): a case study with nanopolystyrene. Sci. Total Environ. 643, 324–334.
Porta, M., Zumeta, E., 2002. Implementing the Stockholm treaty on persistent organic pollutants. vol. 59. BMJ Publishing Group Ltd., pp. 651–652
Priede, I.G., 1985. Metabolic scope in fishes. In: Fish Energetics. Springer, pp. 33–64.
Qiao, R., Deng, Y., Zhang, S., Wolosker, M.B., Zhu, Q., Ren, H., Zhang, Y., 2019. Accumulation of different shapes of microplastics initiates intestinal injury and gut microbiota dysbiosis in the gut of zebrafish. Chemosphere 236, 124334.
Qu, M., Xu, K., Li, Y., Wong, G., Wang, D., 2018. Using acs-22 mutant Caenorhabditis elegans to detect the toxicity of nanopolystyrene particles. Sci. Total Environ. 643, 119–126.
R, 2025. R: A Language and Environment for Statistical Computing. R Foundation for Statistical Computing. https://www.R-project.org/.
Raghunath, A., Perumal, E., 2018. Analysis of lethality and malformations during zebrafish (Danio rerio) development. Methods Mol. Biol. 1797, 337–363. https://doi.org/10.1007/978-1-4939-7883-0_18.
Reidy, S., Kerr, S., Nelson, J., 2000. Aerobic and anaerobic swimming performance of individual Atlantic cod. J. Exp. Biol. 203 (2), 347–357.
Rifai, H., Palachek, R., 2007. Total maximum daily loads for PCBs in the Houston Ship Channel. https://www.tceq.texas.gov/downloads/water-quality/tmdl/houston-ship-galveston-bay-fish-consumption-assessment-78/78-2007-july-quarterly-report.pdf.
Rochman, C.M., Kurobe, T., Flores, I., Teh, S.J., 2014a. Early warning signs of endocrine disruption in adult fish from the ingestion of polyethylene with and without sorbed chemical pollutants from the marine environment. Sci. Total Environ. 493, 656–661. https://doi.org/10.1016/j.scitotenv.2014.06.051.
Rochman, C.M., Lewison, R.L., Eriksen, M., Allen, H., Cook, A.-M., Teh, S.J., 2014b. Polybrominated diphenyl ethers (PBDEs) in fish tissue may be an indicator of plastic contamination in marine habitats. Sci. Total Environ. 476-477, 622–633. https://doi.org/10.1016/j.scitotenv.2014.01.058.
Rowlands, J.C., McEwan, I.J., Gustafsson, J.A., 1996. Trans-activation by the human aryl hydrocarbon receptor and aryl hydrocarbon receptor nuclear translocator proteins: direct interactions with basal transcription factors [Research Support, Non-U S Gov't]. Mol. Pharmacol. 50 (3), 538–548.
Safe, S., Bandiera, S., Sawyer, T., Robertson, L., Safe, L., Parkinson, A., Thomas, P.E., Ryan, D.E., Reik, L.M., Levin, W., et al., 1985. PCBs: structure-function relationships and mechanism of action [Research Support, Non-U S Gov't Research Support, U S Gov't, P H S Review]. Environ. Health Perspect. 60, 47–56.
Sericano, J.L., Wade, T.L., Brooks, J.M., Safe, S.H., 1994. Toxicological significance of non-, mono- and di-ortho-substituted polychlorinated biphenyls in oysters from Galveston and Tampa bays. Environ. Toxicol. Chem. 13 (11), 1797–1803. https://doi.org/10.1002/etc.5620131111.
Sharma, A., Nampoothiri Devadas, V.A., Nair, P.P., Manpoong, C., Kartha, B.D., 2022. Biodegradation of polymers with microbial agents. Curr. Green Chem. 9 (1), 3–13.
Sigler, M., 2014. The effects of plastic pollution on aquatic wildlife: current situations and future solutions. Water Air Soil Pollut. 225 (11), 2184. https://doi.org/10.1007/s11270-014-2184-6.
Sim, Y., Cho, H.-J., Lee, J.-S., Lee, W.S., Kim, H., Jeong, J., 2023. Combined effects of microplastics and benz[a]anthracene on cardiotoxicity in zebrafish (Danio rerio) larvae: size matters. Chemosphere 330, 138723. https://doi.org/10.1016/j.chemosphere.2023.138723.
Singh, B., Sharma, N., 2008. Mechanistic implications of plastic degradation. Polym. Degrad. Stab. 93 (3), 561–584.
Singleman, C., Holtzman, N.G., 2014. Growth and maturation in the zebrafish, Danio rerio: a staging tool for teaching and research. Zebrafish 11 (4), 396–406. https://doi.org/10.1089/zeb.2014.0976.
Singleman, C., Holtzman, N.G., 2021. PCB and TCDD derived embryonic cardiac defects result from a novel AhR pathway. Aquat. Toxicol. 233, 105794. https://doi.org/10.1016/j.aquatox.2021.105794.
Singleman, C., Zimmerman, A., Harrison, E., Roy, N.K., Wirgin, I., Holtzman, N.G., 2021. Toxic effects of polychlorinated biphenyl congeners and aroclors on embryonic growth and development. Environ. Toxicol. Chem. 40 (1), 187–201. https://doi.org/10.1002/etc.4908.
Şişman, T., Geyikoğlu, F., Atamanalp, M., 2007. Early life-stage toxicity in zebrafish (Danio rerio) following embryonal exposure to selected polychlorinated biphenyls. Toxicol. Ind. Health 23 (9), 529–536.
Sleight, V.A., Bakir, A., Thompson, R.C., Henry, T.B., 2017. Assessment of microplastic-sorbed contaminant bioavailability through analysis of biomarker gene expression in larval zebrafish. Mar. Pollut. Bull. 116 (1–2), 291–297.
Somero, G.N., Lockwood, B.L., Tomanek, L., 2017. Biochemical Adaptation: Response to Environmental Challenges, From Life's Origins to the Anthropocene. Sinauer Associates, Incorporated Publishers.
Sørensen, L., Rogers, E., Altin, D., Salaberria, I., Booth, A.M., 2020. Sorption of PAHs to microplastic and their bioavailability and toxicity to marine copepods under co-

exposure conditions. Environ. Pollut. 258, 113844. https://doi.org/10.1016/j.envpol.2019.113844.
Southworth, G., Beauchamp, J., Schmieder, P., 1978. Bioaccumulation potential of polycyclic aromatic hydrocarbons in *Daphnia pulex*. Water Res. 12 (11), 973–977.
Sun, M., Ding, R., Ma, Y., Sun, Q., Ren, X., Sun, Z., Duan, J., 2021. Cardiovascular toxicity assessment of polyethylene nanoplastics on developing zebrafish embryos. Chemosphere 282, 131124.
Takeshita, R., Bursian, S.J., Colegrove, K.M., Collier, T.K., Deak, K., Dean, K.M., De Guise, S., DiPinto, L.M., Elferink, C.J., Esbaugh, A.J., Griffitt, R.J., Grosell, M., Harr, K.E., Incardona, J.P., Kwok, R.K., Lipton, J., Mitchelmore, C.L., Morris, J.M., Peters, E.S., Hall, A.J., 2021. A review of the toxicology of oil in vertebrates: what we have learned following the Deepwater Horizon oil spill. J. Toxicol. Environ. Health B Crit. Rev. 24 (8), 355–394. https://doi.org/10.1080/10937404.2021.1975182.
Tang, J., Ni, X., Zhou, Z., Wang, L., Lin, S., 2018. Acute microplastic exposure raises stress response and suppresses detoxification and immune capacities in the scleractinian coral Pocillopora damicornis. Environ. Pollut. 243, 66–74.
Tanguay, R.L., 2018. The rise of zebrafish as a model for toxicology. Toxicol. Sci. 163 (1), 3–4. https://doi.org/10.1093/toxsci/kfx295.
Tanguay, R.L., 2025. ToxPoint: the indispensable role of zebrafish as a new approach methodology (NAM) in toxicology. Toxicol. Sci. 208 (1), 40–41. https://doi.org/10.1093/toxsci/kfaf121.
Tong, Y., Lin, L., Tao, Y., Huang, Y., Zhu, X., 2023. The occurrence, speciation, and ecological effect of plastic pollution in the bay ecosystems. Sci. Total Environ. 857 (Pt 3), 159601. https://doi.org/10.1016/j.scitotenv.2022.159601.
Toto, B., Refosco, A., O'Keeffe, M., Barkhald, Ø.H., Brønstad, A., Lied, G.A., Yadetie, F., Goksøyr, A., Kögel, T., Dierkes, J., 2022. Intestinal permeability and gene expression after polyethylene and polyamide microplastic ingestion in Wistar rats. Toxicol. Lett. 370, 35–41.
Trevisan, R., Uzochukwu, D., Di Giulio, R.T., 2020. PAH sorption to nanoplastics and the trojan horse effect as drivers of mitochondrial toxicity and PAH localization in zebrafish. Front. Environ. Sci. 8, 78.
Tumwesigye, E., Felicitas Nnadozie, C., C Akamagwuna, F., Siwe Noundou, X., William Nyakairu, G., Odume, O.N., 2023. Microplastics as vectors of chemical contaminants and biological agents in freshwater ecosystems: current knowledge status and future perspectives. Environ. Pollut. 330, 121829. https://doi.org/10.1016/j.envpol.2023.121829.
Ugwu, K., Herrera, A., Gómez, M., 2021. Microplastics in marine biota: a review. Mar. Pollut. Bull. 169, 112540. https://doi.org/10.1016/j.marpolbul.2021.112540.
Ulbrich, B., Stahlmann, R., 2004. Developmental toxicity of polychlorinated biphenyls (PCBs): a systematic review of experimental data. Arch. Toxicol. 78 (5), 252–268.
Umamaheswari, S., Priyadarshinee, S., Kadirvelu, K., Ramesh, M., 2021. Polystyrene microplastics induce apoptosis via ROS-mediated p53 signaling pathway in zebrafish. Chem. Biol. Interact. 345, 109550.
Van den Berg, M., Birnbaum, L.S., Denison, M., De Vito, M., Farland, W., Feeley, M., Fiedler, H., Hakansson, H., Hanberg, A., Haws, L., Rose, M., Safe, S., Schrenk, D., Tohyama, C., Tritscher, A., Tuomisto, J., Tysklind, M., Walker, N., Peterson, R.E., 2006. The 2005 World Health Organization reevaluation of human and mammalian toxic equivalency factors for dioxins and dioxin-like compounds. Toxicol. Sci. 93 (2), 223–241. https://doi.org/10.1093/toxsci/kfl055.
Vandermeulen, J., 1987. Toxicity and sublethal effects of petroleum hydrocarbons in freshwater biota. In: Oil in Freshwater: Chemistry, Biology, Countermeasure Technology, pp. 267–303.
Velzeboer, I., Kwadijk, C.J.A.F., Koelmans, A.A., 2014. Strong sorption of PCBs to nanoplastics, microplastics, carbon nanotubes, and fullerenes. Environ. Sci. Technol. 48 (9), 4869–4876. https://doi.org/10.1021/es405721v.
Verbruggen, E., 2012. Environmental Risk Limits for Polycyclic Aromatic Hydrocarbons (PAHs): For Direct Aquatic, Benthic, and Terrestrial Toxicity.
Wang, J., Tan, Z., Peng, J., Qiu, Q., Li, M., 2016. The behaviors of microplastics in the marine environment. Mar. Environ. Res. 113, 7–17.
Wang, F., Zhang, M., Sha, W., Wang, Y., Hao, H., Dou, Y., Li, Y., 2020. Sorption behavior and mechanisms of organic contaminants to nano and microplastics. Molecules 25 (8), 1827.
Wang, L., Wu, W.-M., Bolan, N.S., Tsang, D.C.W., Li, Y., Qin, M., Hou, D., 2021. Environmental fate, toxicity and risk management strategies of nanoplastics in the environment: current status and future perspectives. J. Hazard. Mater. 401, 123415. https://doi.org/10.1016/j.jhazmat.2020.123415.
Wang, H., Wang, Y., Wang, Q., Lv, M., Zhao, X., Ji, Y., Han, X., Wang, X., Chen, L., 2022. The combined toxic effects of polyvinyl chloride microplastics and di(2-ethylhexyl) phthalate on the juvenile zebrafish (Danio rerio). J. Hazard. Mater. 440, 129711. https://doi.org/10.1016/j.jhazmat.2022.129711.
Wang, H., Wang, Q., Lv, M., Li, J., Zhao, X., Song, Z., Wang, X., You, J., Wang, Y., Chen, L., 2023. Marine micro(nano)plastics determination and its environmental toxicity evaluation. TrAC Trends Anal. Chem. 168, 117332. https://doi.org/10.1016/j.trac.2023.117332.
Wassenberg, D.M., Di Giulio, R.T., 2004. Synergistic embryotoxicity of polycyclic aromatic hydrocarbon aryl hydrocarbon receptor agonists with cytochrome P4501A inhibitors in Fundulus heteroclitus. Environ. Health Perspect. 112 (17), 1658–1664. https://doi.org/10.1289/ehp.7168.
Wei, Z., Wang, Y., Wang, S., Xie, J., Han, Q., Chen, M., 2022. Comparing the effects of polystyrene microplastics exposure on reproduction and fertility in male and female mice. Toxicology 465, 153059.
Wharton, M., Gahn, M.B., Hala, D., Du, J., Park, K., Kaiser, K., 2024. Quantifying Microplastic Contamination in Galveston Bay and the Gulf of Mexico watershed. In: Proceedings of the American Geophysical Union, Ocean Sciences Meeting, New Orleans, LA.
Whyte, J.J., Jung, R., Schmitt, C., Tillitt, D., 2000. Ethoxyresorufin-O-deethylase (EROD) activity in fish as a biomarker of chemical exposure. Crit. Rev. Toxicol. 30 (4), 347–570.
Wickham, H., 2016. ggplot2: Elegant Graphics for Data Analysis, 2nd ed. Springer-Verlag New York. https://doi.org/10.1007/978-3-319-24277-4.
Wickham, H., Vaughan, D., Girlich, M., 2024. tidyr: Tidy Messy Data. Comprehensive R Archive Network (CRAN). https://CRAN.R-project.org/package=tidyr.
Willett, K.L., McDonald, S.J., Steinberg, M.A., Beatty, K.B., Kennicutt, M.C., Safe, S.H., 1997. Biomarker sensitivity for polynuclear aromatic hydrocarbon contamination in two marine fish species collected in Galveston Bay, Texas. Environ. Toxicol. Chem. 16 (7), 1472–1479. https://doi.org/10.1002/etc.5620160721.
Williams, A.K., Bacosa, H.P., Quigg, A., 2017. The impact of dissolved inorganic nitrogen and phosphorous on responses of microbial plankton to the Texas City "Y" oil spill in Galveston Bay, Texas (USA). Mar. Pollut. Bull. 121 (1–2), 32–44.
Winneke, G., Walkowiak, J., Lilienthal, H., 2002. PCB-induced neurodevelopmental toxicity in human infants and its potential mediation by endocrine dysfunction. Toxicology 181, 161–165.
Wright, S.L., Thompson, R.C., Galloway, T.S., 2013. The physical impacts of microplastics on marine organisms: a review. Environ. Pollut. 178, 483–492.
Xu, K., Zhang, Y., Huang, Y., Wang, J., 2021. Toxicological effects of microplastics and phenanthrene to zebrafish (Danio rerio). Sci. Total Environ. 757, 143730. https://doi.org/10.1016/j.scitotenv.2020.143730.
Yang, D., Shi, H., Li, L., Li, J., Jabeen, K., Kolandhasamy, P., 2015. Microplastic pollution in table salts from China. Environ. Sci. Technol. 49 (22), 13622–13627.
Zhang, K., Hamidian, A.H., Tubić, A., Zhang, Y., Fang, J.K.H., Wu, C., Lam, P.K.S., 2021. Understanding plastic degradation and microplastic formation in the environment: a review. Environ. Pollut. 274, 116554.
Zhao, L., Rong, L., Xu, J., Lian, J., Wang, L., Sun, H., 2020. Sorption of five organic compounds by polar and nonpolar microplastics. Chemosphere 257, 127206.
Zhao, L., Shi, W., Hu, F., Song, X., Cheng, Z., Zhou, J., 2021. Prolonged oral ingestion of microplastics induced inflammation in the liver tissues of C57BL/6J mice through polarization of macrophages and increased infiltration of natural killer cells. Ecotoxicol. Environ. Saf. 227, 112882.